Thalamic Network Oscillations Synchronize Ontogenetic Columns in the Newborn Rat Barrel Cortex

Jenq-Wei Yang[1,], Shuming An[1], Jyh-Jang Sun[1], Vicente Reyes-Puerta[1], Jennifer Kindler[1], Thomas Berger[1,2], Werner Kilb[1] and Heiko J. Luhmann[1]

[1]Institute of Physiology and Pathophysiology, University Medical Center of the Johannes Gutenberg University Mainz, Mainz, Germany and [2]Current address: Institute of Physiology, University of Bern, Bern, Switzerland

Address correspondence to Heiko J. Luhmann, Institute of Physiology and Pathophysiology, University Medical Center, Johannes Gutenberg University Mainz, Duesbergweg 6, D-55128 Mainz, Germany. Email: luhmann@uni-mainz.de

J.W.Y. and S.A. contributed equally to this work.

Neocortical areas are organized in columns, which form the basic structural and functional modules of intracortical information processing. Using voltage-sensitive dye imaging and simultaneous multi-channel extracellular recordings in the barrel cortex of newborn rats in vivo, we found that spontaneously occurring and whisker stimulation-induced gamma bursts followed by longer lasting spindle bursts were topographically organized in functional cortical columns already at the day of birth. Gamma bursts synchronized a cortical network of 300–400 μm in diameter and were coherent with gamma activity recorded simultaneously in the thalamic ventral posterior medial (VPM) nucleus. Cortical gamma bursts could be elicited by focal electrical stimulation of the VPM. Whisker stimulation-induced spindle and gamma bursts and the majority of spontaneously occurring events were profoundly reduced by the local inactivation of the VPM, indicating that the thalamus is important to generate these activity patterns. Furthermore, inactivation of the barrel cortex with lidocaine reduced the gamma activity in the thalamus, suggesting that a cortico-thalamic feedback loop modulates this early thalamic network activity.

Keywords: activity dependent, columnar organization, development, in vivo, newborn rat

Introduction

A hallmark of the neocortical architecture is the structural and functional organization in radial units termed cortical columns (Mountcastle 1957; Hubel and Wiesel 1962). In many sensory and motor cortical areas, a cortical column represents the basic module for processing of afferent, intrinsic, and efferent neuronal information (Mountcastle 1997; Jones and Rakic 2010). Cortical columns vary from 300 to 600 µm in diameter depending on the species, cortical area, and on the animal's age and undergo activity- and experience-dependent structural and functional modifications during critical periods (Hensch 2005; Hooks and Chen 2007). A rudimentary pattern of columnar units develops already during early corticogenesis. The "radial unit hypothesis" predicts that progenitors in the ventricular zone of the embryonic cortex produce cohorts of postmitotic neurons that migrate in an inside-first-outside-last pattern along the radial glial cells into the developing cortex forming the early, so-called ontogenetic columns (Rakic 1988; Rakic et al. 2009). This hypothesis has been supported by a number of recent studies demonstrating that proliferative radial glial cells represent the neuronal progenitors (Fishell and Kriegstein 2003) and that clonally related neurons form columnar units in the developing

(Noctor et al. 2001) and mature cortex (Yu et al. 2009). Disturbances in this early development of the columnar architecture may cause disorders in cortical processing associated with neurological deficits such as autism (Amaral et al. 2008) or Fragile X syndrome associated with mental retardation (Bureau et al. 2008; Bureau 2009).

Imaging of intrinsic optical signals and single-unit microelectrode recordings in the primary visual cortex of developing cats have shown that the basic structure of the cortical map for orientation and ocular dominance columns is present at birth and does not depend on visual experience (Crair et al. 1998). Anatomical tracer studies in the visual cortex of newborn ferrets have demonstrated a surprisingly early and rapid development of ocular dominance columns (Crowley and Katz 2000), indicating that molecular cues and/or early neuronal activity guide the initial formation of cortical columns (Katz and Crowley 2002). Neuronal domains of spontaneously coactive neurons coupled through gap junctions and organized in a columnar manner have been demonstrated in the somatosensory cortex of newborn rats in slices (Yuste et al. 1992; Sun and Luhmann 2007) and in intact in vitro preparations of the cerebral cortex (Dupont et al. 2006). However, the role of the neuronal activity in shaping these early columnar networks is not understood. An intrinsic patchy organization of correlated spontaneous activity with a periodicity of ~1 mm, which is in direct relationship with the pattern of early ocular dominance columns, has been demonstrated in the developing visual cortex of ferrets before eye-opening (Chiu and Weliky 2001, 2002). Another source for driving the initial patterning of cortical columnar circuits is the thalamus and the thalamocortical loop. Multi-electrode recordings in the lateral geniculate nucleus of young ferrets revealed patterns of spontaneous activity in the thalamus before eye-opening (Weliky and Katz 1999). Furthermore, a recent study shows that early gamma oscillations enable precise spatiotemporal thalamocortical synchronization in the neonatal rat (postnatal day [P] P2–P7) whisker sensory system (Minlebaev et al. 2011). However, it is not clear to which extent this intrathalamic activity contributes to the generation of spontaneous cortical patterns and the development of functional ontogenetic columns, particularly at an age when cortical layers are still formed (P0–P1 in rats). It is also not known whether spontaneous activity patterns recorded during the early stages of corticogenesis resemble in their spatiotemporal characteristics sensory-evoked responses or whether spontaneous- and sensory-evoked activities represent 2 different entities of the developing cortical network.

We addressed these questions with voltage-sensitive dye imaging (VSDI) and simultaneous multi-channel extracellular electrophysiological recordings in both the barrel cortex and somatosensory thalamus of newborn rats in vivo. Barrel-related columns in the rodent somatosensory cortex represent an ideal model to study the development and the functional organization of a cortical column (Woolsey and Van der 1970). Whiskers on the animal's snout show a well-defined topographic representation in the contralateral ventral posterior medial (VPM) nucleus of the thalamus ("barreloids") and in the so-called barrel field of the somatosensory cortex (Petersen 2007; Fox 2008). This single-whisker to single-column projection allows a selective activation of a barrel-related cortical column in response to specific mechanical stimulation of a single whisker. Furthermore, a barrel-related cortical column can be easily identified with anatomical and physiological techniques (Petersen 2007).

Our simultaneous recordings of spontaneously occurring and whisker stimulation-induced activity in both the thalamus and the barrel cortex following defined mechanical stimulation of a single whisker demonstrate that distinct oscillatory activity patterns synchronize local neuronal networks in a barrel-related cortical column in neonatal rats. Already, shortly after birth, spontaneously occurring and whisker stimulation-induced localized gamma and spindle bursts show a topographic organization in the cortical barrel field. Electrical activation of a single barreloid in the VPM thalamus elicits the gamma/spindle burst pattern in the corresponding cortical barrel and lesioning a thalamic barreloid blocks whisker stimulation-induced and spontaneously occurring cortical gamma bursts, indicating that the thalamus plays an important role in the generation of this early network pattern. Inactivation of the barrel cortex with lidocaine significantly reduced the power in the gamma range of the whisker stimulation-induced and spontaneously occurring thalamic gamma bursts, suggesting that the cortex is modulating the thalamic gamma activity already at the day of birth. Our results demonstrate that the thalamocortical gamma activity synchronizes local cortical networks into ontogenetic columns at early developmental stages, even before the cerebral cortex has achieved its six-layered structure.

Material and Methods

Surgical Preparation

All experiments were conducted in accordance with the national laws for the use of animals in research and approved by the local ethical committee (#23177-07/G10-1-010). In total 95 pups from 65 litters were investigated. VSDI, field potential (FP), and multiple-unit activity (MUA) recordings were performed in the barrel cortex of P0–P7 Wistar rats using experimental protocols similar as described previously (Yang et al. 2009) (Supplementary Fig. S1). Under deep hypothermia combined with an initial light intraperitoneal urethane anesthesia (1 g/kg, Sigma-Aldrich, Taufkirchen, Germany), the animal's head was fixed into the stereotaxic apparatus using one aluminum holder fixed with dental cement on the occipital bones. Depending on the experimental design, the skull was opened in 1 of 2 different ways: 1) For VSDI experiments, a 3×3 mm^2 area of the skull (0–3 mm posterior to bregma and 1.5–4.5 mm from the midline) was thinned on the left hemisphere using a miniature drill until the residual bone, but not the dura mater, above the barrel cortex could be carefully removed with a fine canula and 2) for experiments performing simultaneous multi-channel extracellular electrophysiological recordings in both the thalamus and barrel cortex, a 2×2 mm^2 area of

the skull (in P0–P1 animals: 0–2 mm posterior to bregma and 1.5–3.5 mm from the midline) above the barrel cortex of the left hemisphere was exposed. Additionally another rectangular area (P0–P1: 1–2.5 mm posterior to bregma and 1–2 mm from the midline) of the skull was removed for perpendicular insertion of the thalamic multi-channel electrode. One silver wire was inserted into the cerebellum and served as a ground electrode. The animals were kept at a constant temperature of 37°C by placing them on a heating blanket and covering their bodies with cotton. This experimental set-up allowed VSDI and multi-electrode electrophysiological recordings in light urethane anesthetized animals (<0.2 g/kg) for up to 7 h.

Whisker Stimulation

Single whiskers were stimulated using a protruding device consisting of a miniature solenoid actuator, which was activated by a transistor-transistor logic (TTL) pulse (modified from Krupa et al. 2001). The actuator touched the selected whisker nearby its base and deflected it for 10 ms. The inter-stimulus interval was 20, 30, or 60 s. In most experiments, whiskers were trimmed in order to allow a defined mechanical stimulation of a single whisker.

Voltage-Sensitive Dye Imaging

The VSD RH1691 (Optical Imaging, Rehovot, Israel) was dissolved at 1 mg/ml in a saline solution containing (in mM): 125 NaCl, 2.5 KCl, and 10 HEPES (pH 7.3 with NaOH). The VSD was topically applied to the surface of the barrel cortex and allowed to diffuse into the cortex for 15–30 min. Subsequently, unbound dye was carefully washed away with saline solution. This procedure resulted in a complete staining of all cortical layers from the subplate to the marginal zone/layer I in P0–P1 rats (Supplementary Fig. S2, left) and in a more superficial staining pattern in P6–P7 animals (Supplementary Fig. S2, right), similar to that described previously for the adult rodent cerebral cortex (Berger et al. 2007). The cortex was covered with a 1% low-melting agarose and a cover slip was placed on top to stabilize the tissue. The excitation light from a red LED (MRLED 625 nm, Thorlabs GmbH, Dachau, Germany) was band-pass filtered (630/30 nm) and reflected towards the sample by a 650-nm dichroic mirror. The excitation light was focused onto the cortical surface with a 25-mm Navitar video lens (Stemmer Imaging, Puchheim, Germany). Emitted fluorescence was collected via the same optical pathway, but without reflection of the dichroic mirror, long-pass filtered (660 nm) and focused via another 25-mm Navitar lens onto the chip of a MiCam Ultima L high-speed camera (Scimedia, Costa Mesa, CA, USA). This tandem-type macroscope design (Ratzlaff and Grinvald 1991) resulted in a ×1 magnification. A high-speed camera has a detector of 100×100 pixels, a chip size of 10×10 mm^2, and a field of view of 10×10 mm^2. Using a C-mount extension tube, we reduced the field of view to 2.6×2.6 mm^2 and thereby reduced the vignetting. Every pixel collected light from a cortical region of 26×26 μm^2. The tandem-type macroscope comprising the LED, the filter cube, and the 2 video optics were built in the mechanical workshop of our institute. Fluorescence measurements were synchronized to electrophysiological recordings through TTL pulses.

The spontaneous ongoing activity was detected during 16-s long imaging sessions, while an evoked activity following whisker stimulation was imaged in 2 s long sessions, both with an unbinned whole frame sampling frequency of 500 Hz. For both sets of experiments, data were not averaged.

Evaluation of VSDI Data

Images were analyzed off-line using custom-made routines in the MATLAB software, version 7.7 (Mathworks, Natick, MA, USA). The image data were first processed using a 5×5-pixel spatial binning followed by 60-Hz low-pass filtering to improve the signal-to-noise ratio. Bleaching of fluorescence was corrected by subtraction of a best-fit double-exponential or fifth-degree polynomial (curve-fitting tool in MATLAB). The normalized change of fluorescence intensity ($\Delta F/F_0$) was calculated as the change of fluorescence intensity (ΔF) in each pixel divided by the initial fluorescence intensity (F_0) in the same pixel.

Only fluorescent changes with a maximal $\Delta F/F_0$ of at least 0.2% were considered as evoked responses or spontaneous events. The onset of spontaneous and evoked VSDI responses was defined as the time point when VSDI signals in a 3×3 region were 7 times higher than the baseline standard deviation. The duration of the events was determined when the time in which the signal was above the half-maximal $\Delta F/F_0$ amplitude. The area of the evoked response or spontaneous event was defined as the contour plot of the VSDI response with reference to the half-maximal $\Delta F/F_0$ amplitude. The spatial representation of VSDI responses were displayed according to this threshold. The diameter of the VSDI responses were calculated from the area of the VSDI responses under the assumption of a circular pattern $(d = 2(a/\pi)^{1/2})$.

Multi-Electrode Recording Protocols

Two different types of multi-electrode recordings were performed. 1) After identifying the location of the arc 2 barrels using the VSDI response, an 8-shank 32-channel Michigan-type electrode (1–2 MΩ, NeuroNexus Technologies, Ann Arbor, MI, USA) was inserted in an angle of ~35° into the barrel cortex representing the whiskers of arc 2. The recording sites were separated by 200 or 300 μm in both vertical and horizontal directions (Fig. 3*A*1). In these experiments, we combined imaging and extracellular electrophysiological data acquisition to compare the spatial extent of spindle bursts and activity in the gamma frequency range (20–80 Hz; Wang and Buzsáki 1996; Lahtinen et al. 2002). 2) For simultaneous recordings in both the thalamus and barrel cortex, a 4-shank 32-channel electrode (50 or 100 μm electrode spacing) was labeled with DiI (1,1′-dioctadecyl-3,3,3′,3′-tetramethyl indocarbocyanine, Molecular Probes, Eugene, OR, USA) and inserted into the VPM nucleus of the thalamus. The DiI staining procedure allowed the reconstruction of the electrode tracks in the VPM from postmortem cytochrome oxidase histological sections (Fig. 5*A*2). Another 4-shank 16-channel electrode was inserted into the barrel cortex. Both FP and MUA were recorded for 10 min to 1 h at a sampling rate of 20 kHz using a multi-channel extracellular amplifier and the MC_RACK software (Multi Channel Systems, Reutlingen, Germany).

Electrical Stimulation and Electrolytic Lesion of Single Thalamic Barreloids

For electrical stimulation of single thalamic barreloids, we first identified the recording sites where single-whisker-evoked responses were most prominent (Fig. 7*A*1). The 2 electrodes located nearest to these sites were selected for bipolar electrical stimulation (Fig. 7*A*2). A single current pulse (10–150 μA, 100 μs duration) was applied via a modified MEA1060-Inv-BC preamplifier (Multi Channel Systems) and an isolated stimulation unit (A360, WPI, Sarasota, FL, USA). For electrolytic lesion of the barreloid, an anodal current of 30 μA was applied for 5–10 s via the selected electrodes.

Functional Inactivation of the Barrel Cortex

Pharmacologic inactivation of the barrel cortex was performed via a glass pipette (tip diameter of 30–40 μm) filled with 1% lidocaine hydrochloride monohydrate (Sigma-Aldrich) and attached to a syringe. The tip of the glass pipette was positioned on the barrel cortex surface close to the multi-channel recording electrode. After a 20 min baseline recording, 0.5–1 μL lidocaine was applied. This local inactivation of the barrel cortex lasted approximately for 20 min.

Data Analysis and Statistics

FP recordings were analyzed from the unfiltered data. MUA was detected in 200 Hz high-pass filtered signals by applying a threshold at 5 times the baseline SD. The poststimulus time histograms were computed by summing up the activity in 10–30 trials (10 ms bin size with 1 ms stepwidth) and normalized into the number of multi-unit spikes per second. We defined the following paradigm for the detection of gamma bursts in our data. First, we considered only events with at least 3 periods in the FP and a duration of the first 3 periods of <120

ms, corresponding to an average frequency of >25 Hz. Secondly, the detected gamma burst has to be accompanied by MUA.

Data are presented as mean ± SEM. Statistical analyses were performed with GraphPad Prism (GraphPad Software, Inc.) using the paired *t*-test and Mann–Whitney–Wilcoxon test for paired or un-paired data sets, respectively. The time–frequency spectrogram plots were performed using the Matlab spectrogram function with a time window of 100 ms and an overlapping of 99 ms (Matlab 7.7, Mathworks). Spectrum and coherence analyses were performed using the Chronux toolbox (www.chronux.org). All spectrograms, power spectra, and coherence analyses were performed from unfiltered data. The spectrum of FP, spectrum of MUA, and coherence of FP versus MUA analyses were performed using a time–bandwidth product of TW = 1 with $K = 1$ taper, and the padding factor for the fast fourier transformation (FFT) was 2. The FP coherence between the thalamus and cortex was performed using the time–bandwidth product of TW = 3 with $K = 5$ tapers, and the padding factor for the FFT was 2. The 95% confidence intervals (CIs) were calculated by using the Jackknife method provided in the Chronux toolbox. In all these analyses, the multi-unit spike data were binned at 1 ms.

Results

Precise Topographic Organization of the Sensory Periphery in the Newborn Rat Barrel Cortex In vivo

The cortical response to defined mechanical stimulation of a single whisker was analyzed by in vivo VSDI in the barrel cortex of 39 P0–P7 rats from 22 litters (Fig. 1*A* and Supplementary Fig. S1*A*). At all ages studied, selective stimulation of the C2 whisker evoked in the barrel cortex of the contralateral hemisphere a reliable response, which in all animals allowed the unequivocal identification of the cortical C2-whisker representation (Fig. 1*B*–*D*). The cortical responses to C2-whisker stimulation revealed significant age-dependent differences in their spatial extent, onset latency, and duration. In P0 rats ($n = 7$ from 5 litters), the evoked cortical response was highly localized and revealed an average diameter of 343.1 ± 32.7 μm. The area of the cortical response did not change significantly until P5 ($n = 3$ from 3 litters), when C2-whisker stimulation elicited a response of 491.6 ± 67.2 μm in diameter (Fig. 1*E*). In P6 animals ($n = 4$ from 4 litters), the maximal evoked cortical response often propagated from the initially activated barrel-related column to surrounding columns, and in P7 rats ($n = 6$ from 6 litters), the evoked area increased dramatically to 1436.1 ± 206.5 μm in diameter ($P < 0.01$ in comparison with the P0 age group). The onset latency of the cortical response decreased significantly ($P < 0.01$) from 89.9 ± 8.6 ms at P0 to 35.3 ± 2.8 ms at P7 (Fig. 1*F*). The response duration at the half-maximal amplitude varied from ~240 to ~300 ms in P0–P6 rats and was significantly ($P < 0.05$) shorter in P7 rats only (173 ± 26.4 ms) (Fig. 1*G*).

These results demonstrate that 1) afferent sensory stimulation elicits reliable cortical responses as early as P0, 2) the temporal precision of these cortical responses increases with age, and 3) the spread of the evoked cortical response to neighboring barrel-related columns increases at the end of the first postnatal week.

Spontaneously Occurring Activity Shows a Barrel-Related Columnar Organization

Next we studied with VSDI the spatio-temporal properties of the spontaneous cortical activity in vivo and compared P0–P1 rats with P6–P7 animals, since these 2 age groups showed the
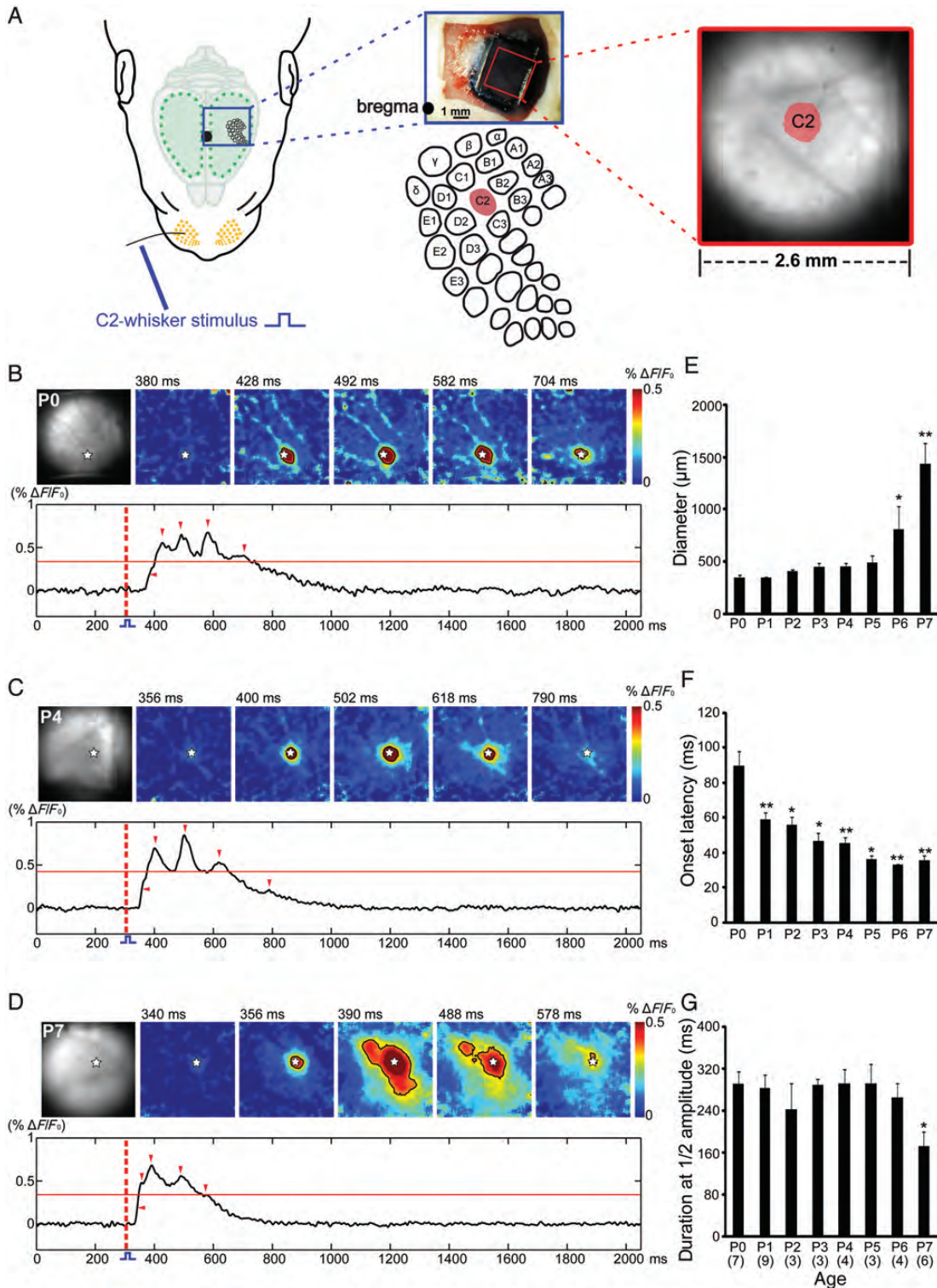
Figure 1. Whisker stimulation elicits a local response in the newborn rat barrel cortex. (*A*) The schematic illustration of the experimental set-up for selective mechanical stimulation of the C2 whisker (left) and simultaneous VSDI in the barrel cortex. The image of the somatosensory cortex stained with the VSD RH1691 (upper middle); the schematic illustration of the barrel-field map with localization of the C2 barrel (lower middle) and microscopic picture of the cortical surface with the evoked response in the C2 barrel-related column after mechanical stimulation of the C2 whisker (right). Black dot indicates bregma position. (*B*–*D*) VSDI in the barrel cortex of a P0 (*B*), P4 (*C*), and P7 (*D*) rat following C2-whisker stimulation at the time point of 300 ms (red-dotted line). The localization of the C2-whisker representation in the barrel cortex and 5 successive poststimulus VSDI responses are shown in the upper rows. White stars indicate the center of the C2-whisker-evoked response. Lower rows show 2-s long optical recordings in which the time points of the 5 successive frames are marked by red arrow heads. Red horizontal line indicates the half-maximal response amplitude. Note the large area of the response in the P7 rat at 390 and 488 ms when compared with the smaller responses in the P0 and P4 rat, where the activity is restricted to the C2 barrel. (*E–G*) Average diameter (*E*), onset latency (*F*), and duration at the half-maximal amplitude (*G*) of the C2-evoked VSDI response in P0–P7 rats. The number of animals is given in parentheses in (*G*). In this and the subsequent figures, the data are expressed as mean ± SEM. Statistical significant differences (Mann–Whitney–Wilcoxon test) versus the P0 age group are indicated by *$P < 0.05$ and **$P < 0.01$.

most significant differences in the evoked cortical activity patterns (Fig. 1*E–G*). In P0–P1 rats, spontaneous events occurred every 4.9 ± 1.7 s and revealed a shorter average duration at the half-maximal amplitude of 247.6 ± 6.4 ms ($P < 0.05$, $n = 317$ events recorded in 5 P0–P1 rats from 5 litters) when compared with the evoked responses (300.8 ± 23.6 ms, $n = 15$ events in the same 5 P0–P1 rats). Spontaneous events covered a cortical area with an average diameter of 387.9 ± 8.3 µm ($n = 317$ events recorded in 5 P0–P1 rats) (Supplementary Movie S1), which was not significantly different from the evoked responses (320.2 ± 11.5 µm, $n = 15$ events in the same 5 P0–P1 rats). These results demonstrate that spontaneous events have very similar spatial properties when the sensory-evoked responses recorded with VSDI at this age. When the spontaneous events were superimposed on the predicted barrel field map of each individual animal, it became evident that 1) 76% of all spontaneous events (241 of 317 events recorded in 5 P0–P1 rats) were located in the barrel field and 2) the large majority of these spontaneous events were restricted to a small cortical region of 300–400 µm in diameter, which resembled in its localization and dimension a single-whisker-defined column (Fig. 2*A*1–4). Since discrete cortical barrels cannot be demonstrated with histological or immunocytochemical methods before P3 (Erzurumlu et al. 1990), we refer to these early neuronal networks as functional pre-barrel-related columns or functional pre-columns. In P0–P1 rats ($n = 14$ from 12 litters), 70–80% of the spontaneous events were localized in 1 or 2 pre-barrel-related columns and ~20% in 3–6 pre-columns (Fig. 2*A*4–6,*C*). In this age group, the spontaneously occurring activity only rarely covered an area of >6 pre-barrel-related columns. In P6–P7 rats, spontaneous events ($n = 462$ in 15 animals from 11 litters) occurred every 2.6 ± 0.2 s ($P < 0.05$ vs. P0–P1), revealed an average duration at the half-maximal amplitude of 184 ± 6.6 ms ($P < 0.001$), and 77% of them were located in the barrel field (Fig. 2*B*1–3). As in P0–P1 rats, ~70% of the spontaneous events recorded in P6–P7 animals covered only 1 or 2 barrel-related columns (Fig. 2*B*4). About 20% of the events were localized in 3–6 columns and ~10% in >6 barrel-related columns (Fig. 2*B*5–6,*C* and Supplementary Movie S2).

These results demonstrate that 1) in the newborn (P0–P1) rat barrel cortex spontaneous events are predominantly restricted to single pre-barrel-related columns, 2) these spontaneous events have similar properties as sensory-evoked cortical responses, and 3) at the end of the first postnatal week spontaneously occurring activity may spread from the initially activated pre-barrel-related column to numerous neighboring columns.

Local Network Bursts Mediate the Activation of Cortical Pre-Columns

In order to characterize in more detail the mechanisms underlying the whisker stimulation-induced and spontaneously occurring optical activity patterns, we performed simultaneous VSDI and multi-electrode extracellular recordings in 3 P1 rats from 3 litters in vivo (Fig. 3*A*1 and Supplementary Fig. S1*A*). After identification of the cortical C2 barrel by selective mechanical stimulation of the C2 whisker and simultaneous VSDI, an 8-shank 32-channel electrode was inserted at an angle of ~35° into the cortex at the site of the C2 barrel (Fig. 3*A*2, left). In good agreement with the VSDI response, the
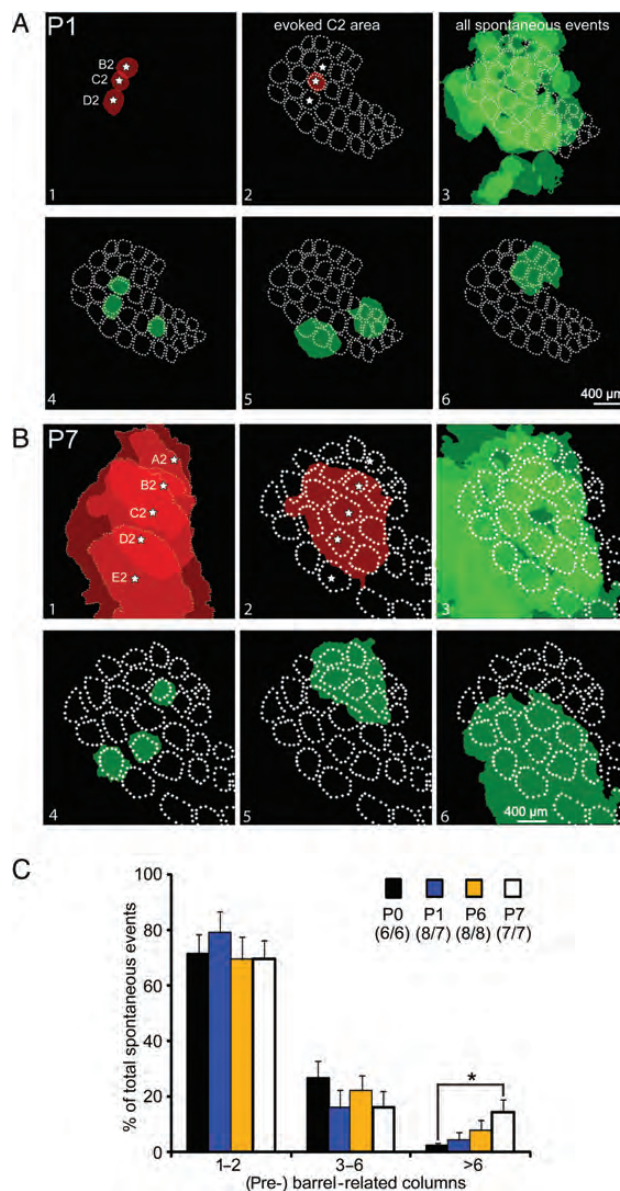
Figure 2. Spontaneously occurring activity assembles barrel-related columnar networks. (*A,B*) Spontaneously occurring and whisker stimulation-induced activity recorded in the somatosensory cortex of one P1 (*A*) and one P7 (*B*) rat. Color-coded spots represent the area of evoked VSDI responses or spontaneous VSDI events with at least half-maximal $\Delta F/F_0$ amplitude. Panel 1 shows the cortical representation of 3 or 5 whiskers of arc 2 as determined by selective mechanical stimulation of a single whisker. White star marks the center of each activated barrel. Panel 2 illustrates the response to C2-whisker stimulation in the map of the whole barrel field. A barrel field map was generated on the basis of a cytochrome oxidase stained horizontal section and aligned according to the evoked responses. In panel 3, all spontaneous events ($n = 75$ in [*A*] and $n = 71$ in [*B*]) recorded in this P1 or P7 rat are superimposed on the barrel field map. Single spontaneous events localized in a single (pre-) barrel-related column (panel 4) or in more than one (pre-)barrel-related column (panels 5 and 6) are shown. (*C*) The percentage distribution of spontaneous events, which are restricted to 1–2, 3–6, or >6 (pre-)barrel-related columns. The number of animals/litters investigated for in each age group is given in parentheses. Statistical significant differences (Mann–Whitney–Wilcoxon test) versus the P0 age group are indicated by *$P < 0.05$.

electrophysiological response to C2-whisker stimulation also consisted of a rather localized activity (Fig. 3*A*2, right). When all 8-shank recording electrodes (S1–S8) were positioned in an appropriate manner, the stimulus-evoked
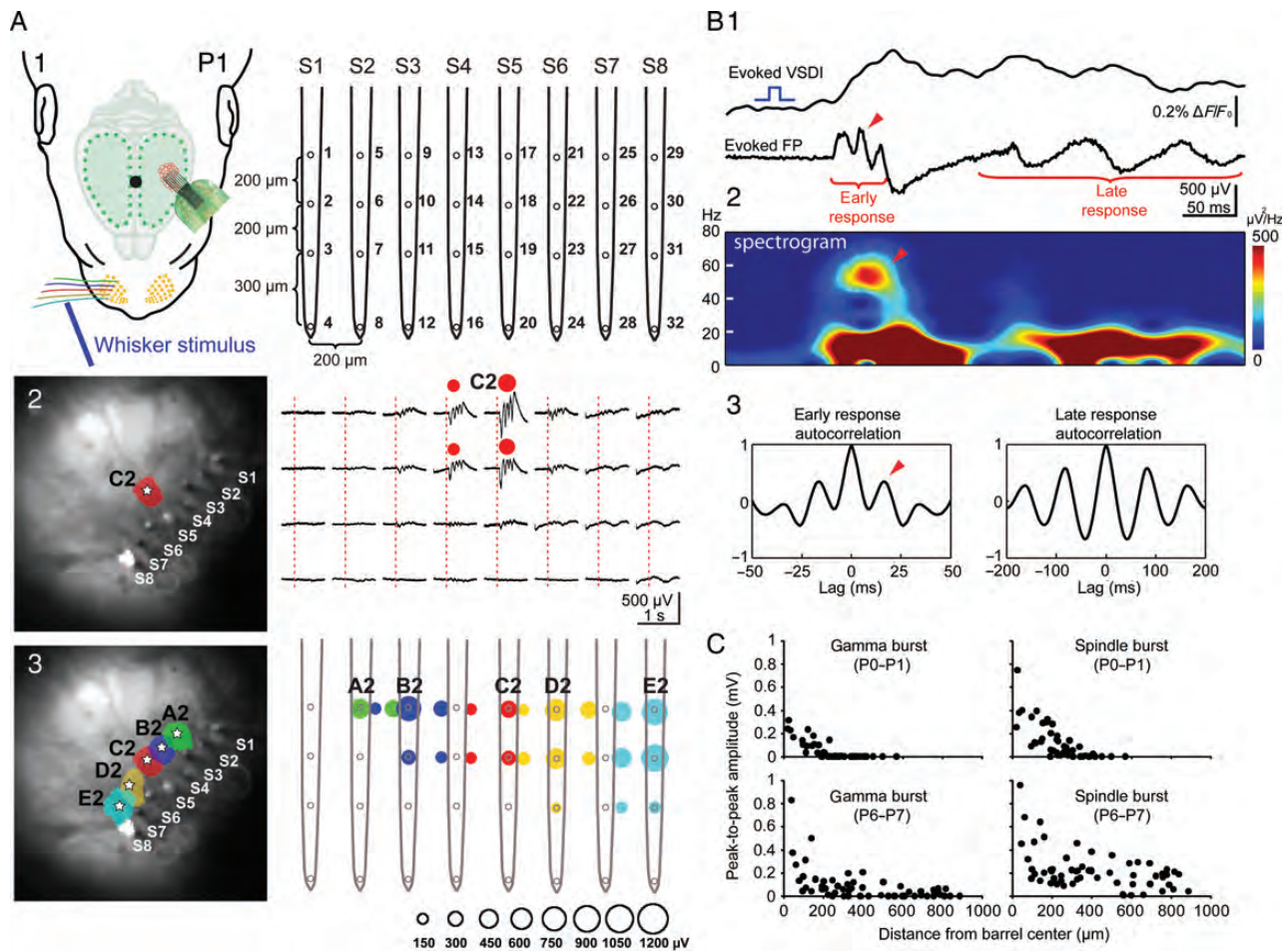
Figure 3. Gamma and spindle bursts synchronize functional cortical columns. (A) The simultaneous VSDI and the multi-electrode recording of stimulus evoked the local cortical responses. The schematic illustration of the experimental set-up combining selective single-whisker stimulation, VSDI, and cortical 32-channel recordings using an 8-shank electrode (S1–S8) with shank spacing of 200 μm (A1). Mechanical stimulation of the C2 whisker in a P1 rat elicits a local VSDI (left) and local electrophysiological (right) response in the C2 barrel (A2). Color-coded localization of the evoked cortical VSDI (left) and electrophysiological (right) responses to stimulation of single whiskers in arc 2 (A3). The first negative peak amplitude of the electrophysiological response corresponds to the size of the color-coded circles as shown below the graph. Ten times baseline standard deviation was used as the threshold (~150 μV) to define the spatial extent of the electrical response. (B) VSDI and FP response recorded simultaneously in the cortical E2 barrel following mechanical stimulation of the E2 whisker in a P1 rat. The corresponding spectrogram plot of the evoked FP response and autocorrelograms of early- and late-evoked FP response are shown below. Note the the early response with a period of ~20 ms (arrowheads in B1–3) corresponding to a ~50-Hz gamma burst discharge, while the late component showed a slower frequency. (C) The relationship between the peak-to-peak amplitude and the distance from the center of the (pre-) barrel-related column for evoked gamma bursts (left) and spindle bursts (right) in P0–P1 (upper panels, $n = 44$ recordings in 4 animals from 4 litters) and P6–P7 rats (lower panels, $n = 59$ recordings in 5 animals from 4 litters).

electrophysiological responses depicted the topographic cortical representation of the 5 single arc 2 whiskers, namely A2 to E2 (Fig. 3A3). Similar to the evoked response recorded in the C2 barrel, single-whisker stimulation of the A2, B2, D2, or E2 whisker also elicited a local VSDI and electrophysiological response that was organized in a topographic manner. These experiments also demonstrated a close correlation of the FP responses with the VSDI responses in their location and spatial extent.

The previous electrophysiological studies in both the newborn rat barrel cortex demonstrated 2 main types of spontaneously occurring and stimulus-evoked network activity patterns: 1) short-lasting gamma oscillations and 2) longer spindle bursts with a frequency of ~10 Hz (Minlebaev et al. 2007; Yang et al. 2009). Our VSDI and simultaneous multichannel extracellular recordings demonstrate that both types of electrophysiological activity patterns contribute to the optical signal (Fig. 3B1). Following mechanical stimulation of

a single whisker, the early FP response consisted of a short lasting burst in the gamma-frequency band (20–80 Hz; Wang and Buzsáki 1996; Lahtinen et al. 2002) and was correlated with the rising phase of the optical signal, indicating that the gamma activity plays an important role in synchronizing the pre-column network. This initial gamma activity was followed by a typical spindle burst as described previously (Minlebaev et al. 2007, 2009; Yang et al. 2009). Although in 11% of the experiments ($n = 7$ of 65 events recorded in 13 P0–P1 rats from 12 litters), a pure gamma burst could be observed, in most cases, the gamma activity was followed by a spindle burst ($n = 56$). Only 2 of 65 events (3%) recorded in P0–P1 rats were pure spindle bursts without the gamma activity. Both the spectrogram and the autocorrelation analyses revealed a clear gamma activity in the early response and the characteristic ~10-Hz frequency in the subsequent spindle burst (Fig. 3B2,3). When the peak-to-peak amplitude of the evoked response was plotted against its distance to the center

of the barrel as identified by VSDI, it became evident that gamma bursts in P0–P1 rats are spatially confined to an area of ~400 µm in diameter, whereas spindle bursts cover larger areas of ~600 µm in diameter (upper panels in Fig. 3C). In agreement with our previous VSDI data, the spatial extent of the electrophysiological responses became larger with increasing age (lower panels in Fig. 3C).

When in P0–P1 rats, the stimulus-evoked cortical FP response was compared with the corresponding MUA, a clear relationship between both signals could be detected (Fig. 4A). This correlation became more evident in the average power spectrum and coherence analyses of the evoked FP responses and MUA ($n = 56$ events recorded in 9 P0–P1 rats from 8 litters). The averaged FP and MUA response of the gamma burst revealed a clear peak at the frequency of 40–50 Hz, which was also evident in the coherence plot of the FP versus MUA (Fig. 4B1). A correlation between FP and MUA could also be demonstrated for the spindle bursts, which revealed a peak at the frequency of ~10 Hz (Fig. 4B2).

These results demonstrate that 1) gamma and spindle bursts are the electrophysiological activity patterns underlying the local VSDI signals evoked by single-whisker stimulation, 2) short-lasting gamma activity precedes the spindle burst, 3) gamma bursts in P0–P1 rats synchronize a pre-barrel-related column of ~400 µm in diameter, and 4) the neuronal discharges correlate with the synchronized FP responses.

Thalamic Activity Elicits Local Cortical Bursts

In order to study the functional role of the thalamus in the generation of sensory-evoked cortical oscillations, we performed multi-channel extracellular recordings in the VPM nucleus of the thalamus in newborn rats in vivo (Fig. 5A1). The tracks of the DiI-labeled electrodes were subsequently reconstructed in histological sections to allow identification of the thalamic recording sites (Fig. 5A2). As in the barrel cortex, single-whisker stimulation elicited a local thalamic FP response that was accompanied by MUA (Fig. 5A3) and which consisted of an early brief component with the gamma activity and a slower late response (Fig. 5A4). In all recordings from P0 to P1 rats, the early gamma activity in the FP responses correlated with the local MUA (Fig. 5B). This correlation could clearly be demonstrated in the average power spectrum and coherence analyses of the evoked FP and MUA responses, which revealed a peak at 40–50 Hz ($n = 10$ P0–P1 rats from 7 litters) (Fig. 5C). These data demonstrate that the thalamus generates gamma burst activity in the newborn rat in vivo upon sensory stimulation.

In order to study the relation between sensory-evoked thalamic burst activity and cortical gamma bursts, we performed simultaneous multi-channel extracellular recordings in both the VPM nucleus of the thalamus and barrel cortex (Fig. 6A). From a total of 1088 thalamic and 544 neocortical recording sites in 29 P0–P1 rats from 22 litters, we found upon mechanical single-whisker stimulation only 14 functional thalamocortical connections showing clear gamma bursts in both the thalamus and cortex. This low connectivity rate can be explained by the fact that in contrast to the cortical VSDI-guided recordings, the thalamic multi-electrode recording does not allow an a priori identification of the whisker representation. The transfer of sensory information from the VPM thalamus to the barrel cortex was surprisingly reliable already in P0–P1

rats, showing no failures (data not shown). In P0–P1 rats, the early thalamic gamma response had a stimulus-to-onset latency of 36.7 ± 1.7 ms, a duration of 92.3 ± 2.7 ms and was followed by a late response of 710.8 ± 53.6 ms in duration ($n = 14$ connections in 13 animals) (Fig. 6B). The early cortical gamma burst had an onset latency of 56.1 ± 2.5 ms, a duration of 89.1 ± 3.7 ms and was followed by a spindle burst of 644.5 ± 44.5 ms in duration ($n = 14$ connections in 13 animals). The thalamocortical transfer in P0–P1 rats required 19.3 ± 0.9 ms, which was also evident in the cross-correlogram of the early MUA responses (Fig. 6C1). Furthermore, the early response showed significant coherence between the thalamus and the cortex in the gamma frequency range (Fig. 6C2).

Further, the proof for the role of the thalamus in generating the cortical gamma activity in newborn rats came from experiments in which the VPM was locally activated by bipolar electrical stimulation and the resulting cortical response was recorded with a multi-channel electrode. The thalamic stimulation site was identified by responses to single-whisker stimulation in simultaneous 32- and 16-channel recordings in both the thalamus and barrel cortex, respectively (Fig. 7A1). When the thalamic recording site showing the maximal response to whisker deflection was activated via bipolar electrical stimulation, a cortical response very similar to the sensory-evoked response could be observed in the corresponding pre-barrel-related column (Fig. 7A2,B). The duration (84.9 ± 3.8 ms) and frequency (37.7 ± 2.1 Hz) of the cortical gamma bursts evoked by barreloid electrical stimulation was not significantly different compared with the sensory-evoked gamma bursts (89.3 ± 8.6 ms and 41.8 ± 3.2 Hz, respectively, $n = 7$ P1 rats from 7 litters). These results demonstrate that electrical stimulation of the thalamus is capable of eliciting a cortical response that resembles the cortical activity pattern evoked by mechanical stimulation of a single whisker. In contrast, bipolar electrical stimulation of a site located 400 µm above or 200 µm aside of the barreloid elicited no clear response at any of the 16 cortical recording sites (Fig. 7A3), demonstrating that the stimulation protocol activated only a small region of thalamic tissue.

Our data demonstrate that 1) the thalamocortical projection reliably transfers the sensory information from the whisker to the barrel cortex as early as P0–P1, 2) thalamic gamma bursts are capable of driving local gamma bursts in the barrel cortex following single-whisker stimulation in P0–P1 rats, and 3) the thalamic activity is sufficient to trigger local gamma bursts in the barrel cortex.

The Thalamus Is Important for the Generation of Spontaneously Occurring Cortical Bursts

Next we addressed the question whether the local spontaneously occurring activity observed in the barrel cortex of P0–P1 rats with VSDI (Fig. 2) requires the thalamic activity or whether it is generated independently from the thalamus by intracortical mechanisms. The average occurrence of spontaneous cortical spindle bursts (gamma-containing and pure spindle bursts grouped together) was 0.9 ± 0.2 min^{-1} ($n = 6$ in P0–P1), which is ~35% of the results of Minlebaev et al. (2007) (2.5 ± 0.4 min^{-1} in P2–P7 rats) and Marcano-Reik et al. (2010) (~40/15 min, equal to 2.7 min^{-1} in P2–P6 rats). The lower occurrence of spindle bursts in our data might be due to age differences, since we focused on the P0–P1 age group.
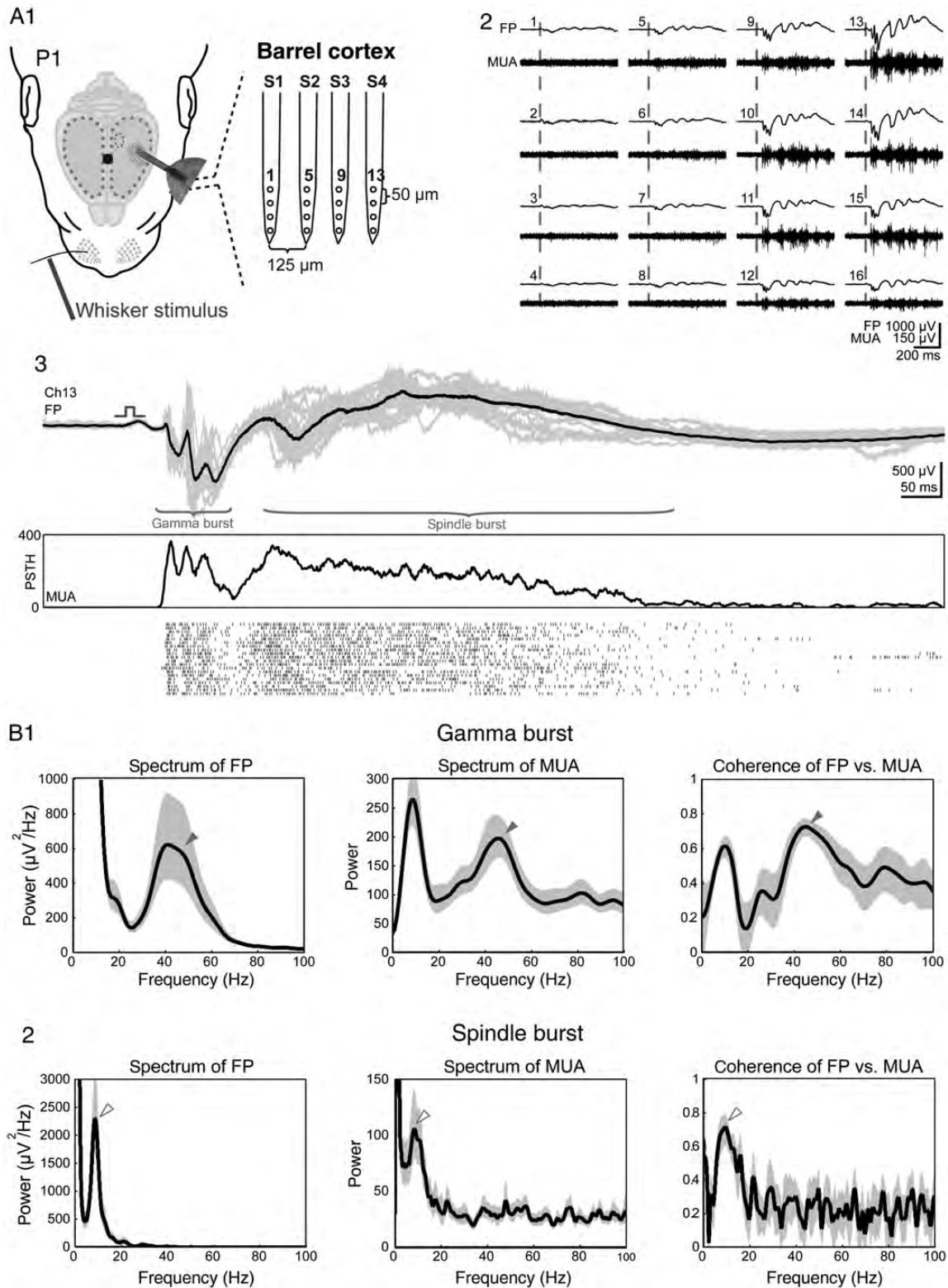
Figure 4. Cortical bursts correlate with MUA. (*A*) FP and multi-unit recordings of single-whisker-evoked responses in the barrel cortex. The schematic illustration of the experimental set-up with a 4-shank 16-channel electrode (*A*1). FP (upper traces) and MUA responses (lower traces) to single-whisker stimulation recorded in a P1 rat with the electrodes shown in panel 1 (*A*2). Average (black trace) and superimposed 20 single (shaded area) cortical FP responses and corresponding poststimulus time histogram (PSTH) of 20 succeeding whisker stimulations every 20 s (*A*3). Note the presence of gamma activity in the early response in the FP and MUA. (*B*) Average spectrum and coherence analyses of evoked gamma burst (*B*1) and spindle burst (*B*2) responses recorded in 9 P0–P1 rats. Black traces show averages and the shaded area represents the 95% CI. Note the prominent 40–50 Hz activity in the averaged gamma burst (filled arrowheads) and ~10 Hz peak in the spindle burst response (open arrowheads). Shaded areas in (*B*) represent 95% CI.
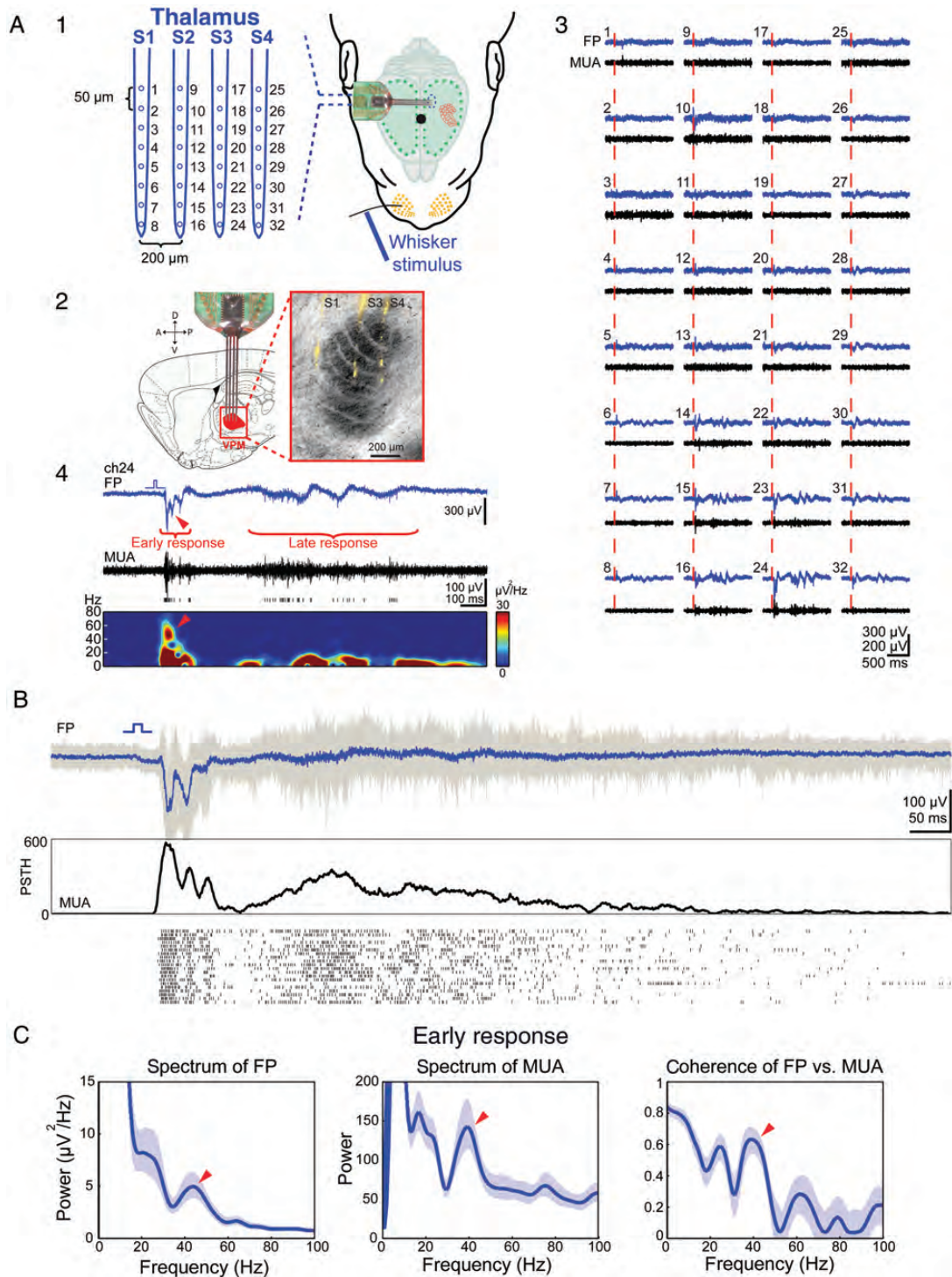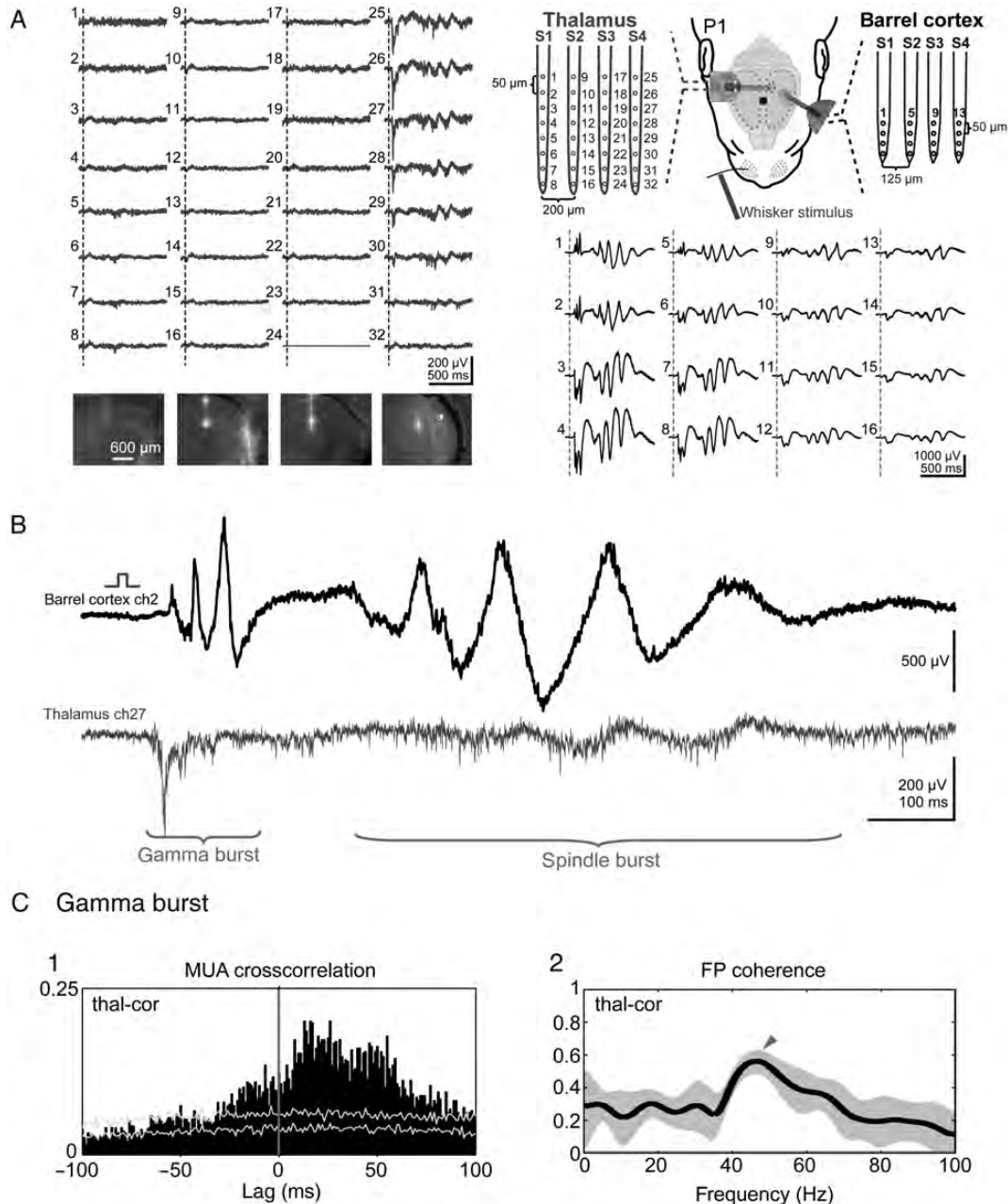
Figure 5. Whisker stimulation elicits gamma activity in the thalamus. (*A*) Electrophysiological recordings of the whisker-evoked FP and MUA responses in the thalamic VPM of the newborn rat. The schematic illustration of the experimental set-up with a 4-shank 32-channel electrode located in the thalamus (*A*1). The schematic illustration of a sagittal brain section showing the location of the recording electrodes in the VPM thalamus (left picture taken from Paxinos and Watson 1998) (*A*2). The image of cytochrome oxidase stained section from the newborn rat showing 3 Dil-stained electrode tracks S1, S3, and S4 (right). Representative thalamic responses to single-whisker stimulation recorded with multi-electrode S1–S4 in a P0 rat (*A*3). The enlargement of response recorded at channel 24 with the corresponding spectrogram plot (*A*4). Note the gamma component in early response (arrowhead in *A*4). (*B*) Average (blue trace) and 20 superimposed single (shaded area) FP responses with corresponding poststimulus time histogram (PSTH) of 20 succeeding whisker stimulations every 30 s in a P1 rat. (*C*) Average spectrum and coherence analyses of evoked early thalamic responses recorded in 10 P0–P1 rats. Note the prominent gamma activity in the averaged FP and MUA spectrum and in the coherence plot (arrowheads). Shaded areas in (*C*) represent 95% CIs.

In all 14 simultaneous recordings with a functional thalamocortical connection from 13 P0–P1 rats (12 litters), we observed spontaneously occurring activity (Fig. 8A).

Spontaneously occurring activity in the barrel cortex consisted only in 52% of all events (n = 146 of 280 events) of an initial gamma component followed by a spindle burst

Figure 6. Whisker stimulation evoked cortical gamma bursts are preceded by the local thalamic activity. (*A*) Simultaneous multi-channel recordings of sensory-evoked responses to single-E5-whisker stimulation in both the VPM thalamus and barrel cortex of a P1 rat. The schematic illustration of the experimental set-up with a 4-shank 32-channel electrode located in the thalamus (blue) and a 4-shank 16-channel electrode in the cortex (black). The images show electrode tracks of the 4 Dil-stained electrodes S1–S4 in the thalamus. (*B*) Whisker stimulation evoked gamma and spindle burst response recorded simultaneously with cortical channel 2 and thalamic channel 27 in the P1 rat. (*C*) Cross-correlation of the MUA (*C1*) and coherence analysis (*C2*) of 20 evoked FP responses recorded simultaneously in both the thalamus and barrel cortex. Note that the thalamic MUA precedes cortical MUA (*C1*) and that the FP coherence plot reveals a clear gamma component (arrowhead in *C2*). Shaded area in *C2* represents 95% CI.

(Fig. 8*A*). Twenty percent (57 of 280 events) showed only the initial gamma component and 28% (77 of 280 events) were pure spindle bursts without any obvious gamma activity, in contrast to the stimulus-evoked responses (11% pure gamma burst and 3% pure spindle bursts). Similar to the VSDI data, the duration of spontaneously occurring activity was also shorter than that of evoked responses (496.1 ± 19 ms, $n = 280$ events and 735.8 ± 17.3 ms, $n = 140$ events, respectively, $P < 0.001$). All spontaneous cortical events ($n = 280$) were preceded by the thalamic activity (Fig. 8*B*).

Next we focused on those spontaneous events containing gamma bursts. The power spectrum analyses of the spontaneous gamma burst activity in both the cortex and thalamus showed a prominent peak at 30–40 Hz in FP and MUA recordings (Fig. 8*C*1,2). The synchronization of spikes in this frequency band is also evident in the coherence plot of FP versus MUA recordings in both the cortex and the thalamus (Fig. 8*D*). Finally, the promi-nent FP coherence between the cortex and thalamus at 30–40 Hz (Fig. 8*E*2) is also similar between spontan-eously occurring and whisker stimulation-induced gamma bursts.
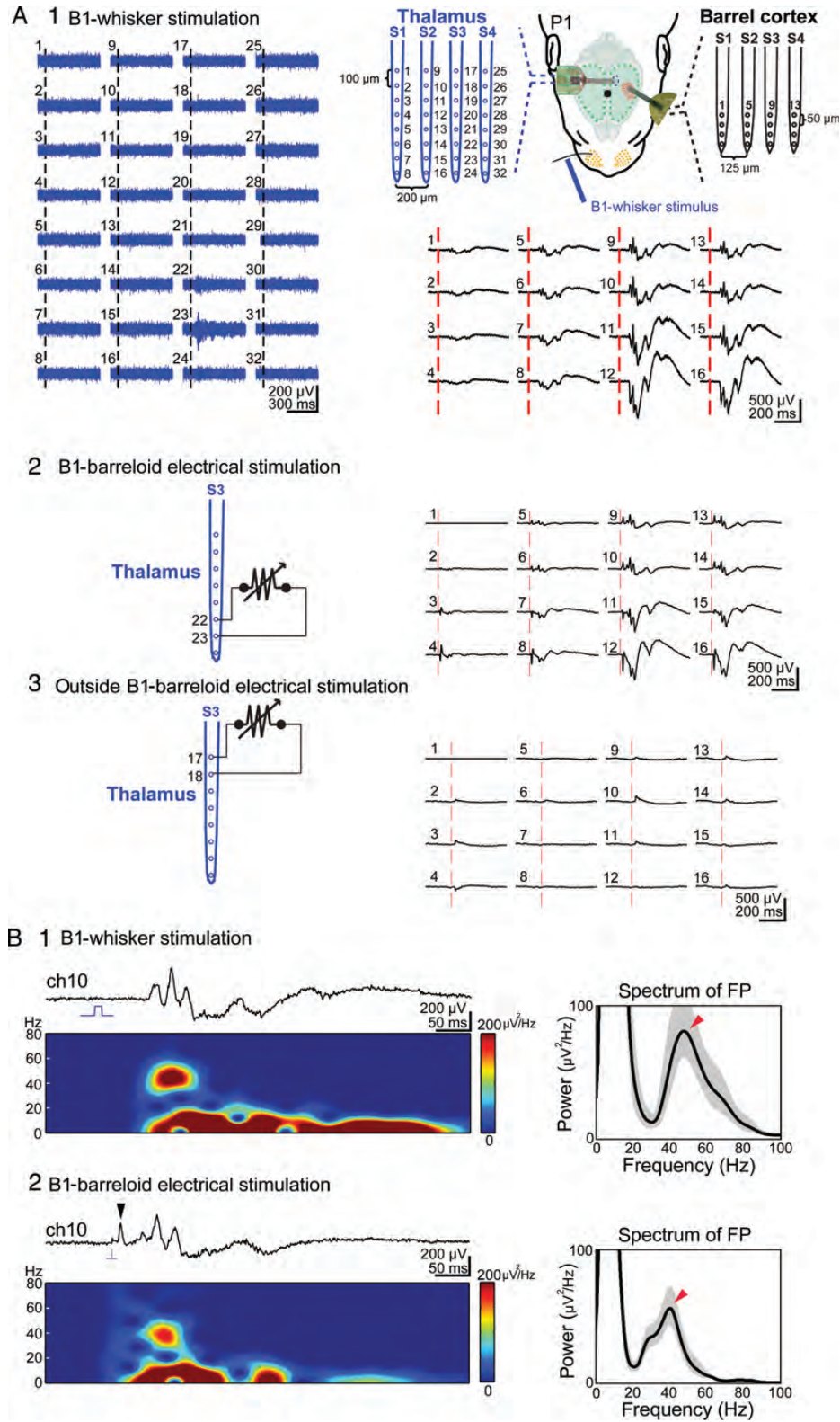
Figure 7. Local electrical stimulation of the thalamus elicits cortical gamma and spindle bursts. (*A*) Simultaneous multi-channel recordings of the thalamic (blue traces) and cortical responses (black traces) to B1-whisker stimulation in a P1 rat (*A1*). The schematic illustration of the experimental set-up with a 4-shank 32-channel electrode located in the thalamus (blue) and a 4-shank 16-channel electrode in the barrel cortex (black) is shown in the upper right panel. Note that the thalamic MUA responses to B2-whisker stimulation are located at channels 22 and 23. Bipolar electrical stimulation (120 µA, 100 µs duration) of the B1 thalamic barreloid at channels 22 and 23 elicits the local cortical responses in the B1 barrel (*A2*). No cortical responses were elicited when the electrical stimulation was performed outside the B1 thalamic barreloid (*A3*). (*B*) The cortical responses recorded at electrode number 10 to B1-whisker stimulation (*B1*) and thalamic B1 barreloid (*B2*) electrical stimulation. Both responses reveal a prominent gamma component in spectrogram and FP spectrum analysis (marked by the arrowheads). Note the antidromic population spike (arrowhead) upon thalamic stimulation. Shaded areas in right panels of (*B*) represent 95% CI.
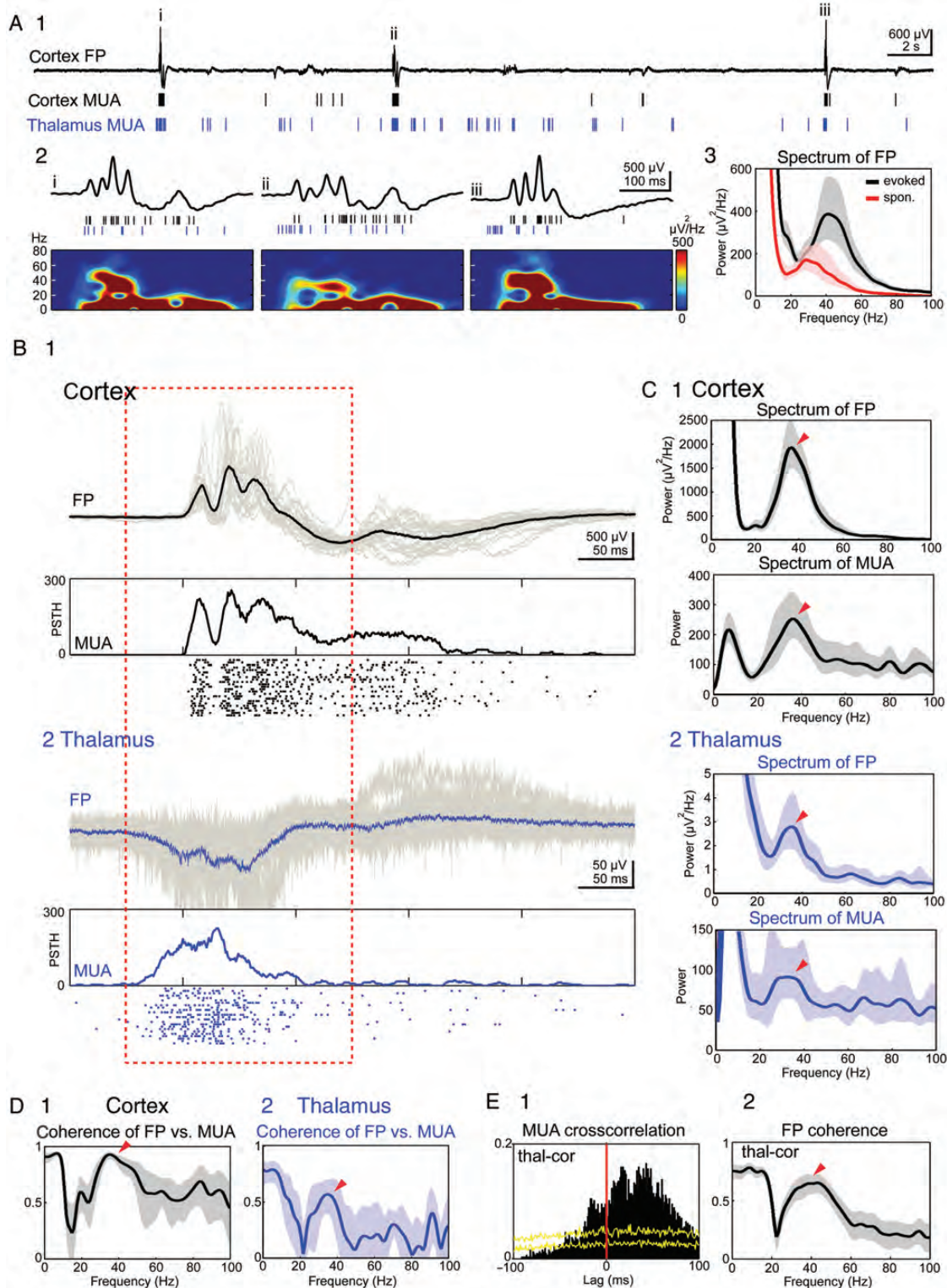
Figure 8. The spontaneous cortical gamma activity arises in the thalamus. (*A*) Simultaneous 40 s recording of spontaneously occurring activity in the barrel cortex and VPM thalamus of a P1 rat. Upper trace represents the cortical FP recording; cortical (black bars) and thalamic MUA (blue bars) are presented below (*A*1). The 3 spontaneous events i–iii marked in *A*1 are shown at higher resolution with corresponding spectrograms (*A*2). Note the gamma activity in (i) and (iii). An averaged spectrogram of 140 evoked (black) and 140 spontaneous (red) cortical gamma bursts in 14 simultaneous recordings with a functional thalamocortical connection from 13 P0–P1 rats (*A*3). Shaded areas represent 95% CI. (*B*) Average (black trace) and 24 superimposed single (shaded area) spontaneous FP events and MUA recorded simultaneously in the cortex (*B*1) and in the thalamus (*B*2). Thalamic and cortical recordings were aligned to the onset of the cortical spontaneous FP events. (*C*) Spectrum analyses of the cortical (*C*1) and thalamic (*C*2) spontaneous FP and MUA events shown in (*B*). (*D*) Coherence analyses of spontaneous FP events versus MUA recorded simultaneously in the cortex (*D*1) and thalamus (*D*2). (*E*) Cross-correlation of the spontaneous MUA (*E*1) and coherence analysis of the FP (*E*2) recorded simultaneously in the thalamus and barrel cortex. Arrowheads in (*C*–*E*) point to the gamma component. Diagrams in (*C*–*E*) were calculated from the data marked by red dashed line in (*B*). Shaded areas in (*C*–*E*) represent 95% CI.

However, the spontaneously occurring gamma bursts recorded in both the thalamus and cortex of P0–P1 rats differed from the whisker stimulation-induced responses obtained at the same recording sites. The thalamic spontaneously occurring activity had a longer duration (134.9 ± 6.1 ms, $P < 0.001$, $n = 14$ connections in 13 P0–P1 rats, paired t-test) and slower frequency (33.4 ± 1.3 Hz, $P < 0.001$) when compared with the sensory-evoked thalamic responses (92.3 ± 3.9 ms and 40.2 ± 1.7 Hz, respectively). Cortical spontaneous gamma bursts also had a longer duration of 120.1 ± 4.8 ms ($P < 0.001$) and a slower frequency of 32.3 ± 1.1 Hz ($P < 0.01$) when compared with the sensory-evoked cortical responses (89.1 ± 5.5 ms and 39.1 ± 2.3 Hz, respectively) (Fig. 8A3). Finally, the thalamocortical transfer of spontaneously occurring activity was slower (36.2 ± 2 ms) than that of sensory-evoked responses (19.3 ± 1.1 ms, $P < 0.001$), as it is also evident from the MUA cross-correlation (Fig. 8E1). However, despite these differences, these data demonstrate that spontaneous gamma bursts in the cortex are closely linked to the thalamic activity patterns.

To directly address the question, whether the thalamus plays a critical role in generating spontaneous cortical bursts, we analyzed the functional consequences of acute local inactivation of the thalamus on the expression of sensory-evoked and spontaneous cortical bursts recorded in the barrel cortex of P0–P1 rats. Simultaneous multi-electrode recordings in both the VPM and barrel cortex upon single-whisker stimulation (control in Fig. 9A1) were used to determine the site of thalamic lesion. Since the thalamic high-density recordings allowed the unequivocal identification of the activated barreloid (cf. Fig. 7A1), the thalamic representation of the stimulated whisker could be locally inactivated by an electrolytic lesion (Fig. 9A4). Following this local thalamic lesioning, single-whisker stimulation elicited, as expected, no longer any kind of activity in the thalamus and only small sensory-evoked responses in the cortex (Fig. 9A2). When compared with the cortical MUA responses obtained before the local thalamic inactivation, the average number of spikes and the power of the gamma spectrum in the early response, which corresponds to the gamma burst phase, were significantly reduced to $11.4 \pm 5.3\%$ and $8.2 \pm 4.6\%$, respectively ($n = 6$ P0–P1 rats from 6 litters, Fig. 9A3). In addition, the number of spikes and the power of the MUA spectrum (<20 Hz) in the late response, which corresponds to the spindle burst phase, were also significantly reduced to $2.6 \pm 1.3\%$ and $2.6 \pm 1.6\%$, respectively ($n = 6$ P0–P1 rats, Fig. 9A3). In summary, these results demonstrate that VPM lesions virtually abolished the cortical responses evoked by whisker stimulation.

In addition, this local inactivation of the thalamus massively attenuated spontaneously occurring cortical activity (Fig. 9B1,2). While both pure gamma bursts and gamma containing spindle bursts were completely abolished, a few pure spindle bursts could still be observed in 4 of the 6 lesioned animals, however, with a significantly ($P < 0.05$) reduced occurrence of only 0.1 ± 0.05 min^{-1} (Fig. 9B4). The total number of spikes within bursts was reduced to $1.3 \pm 0.9\%$ ($n = 6$ P0–P1 rats, Fig. 9B3). Accordingly, the power of the gamma spectrum was also abolished ($2.8 \pm 1.8\%$, Fig. 9B3). In summary, these results demonstrate that the thalamic VPM is critically involved in the generation of the spontaneous cortical gamma and spindle burst activity, which synchronizes developing cortical networks into functional pre-barrel-related columns. Only a small portion of remaining spontaneous pure spindle

bursts may originate in the barrel cortex itself, in adjacent cortical areas or in non-thalamic subcortical structures.

Modulation of Thalamic Gamma Bursts by Cortico-Thalamic Feedback

In order to study a potential cortico-thalamic feedback modulation of the thalamic network activity, the cortex of P0–P1 rats was inactivated by the surface application of 1% lidocaine. Mechanical stimulation of a single whisker elicited the typical response in the VPM and barrel cortex (Fig. 10A1). After lidocaine application, the cortical responses were, as expected, completely blocked (Fig. 10A2), while the thalamic activity could be clearly seen. However, in all 7 animals from 6 litters, the cortical inactivation desynchronized the activity in the corresponding barreloid. No obvious gamma peak was observed in the thalamic MUA spectrograms (Fig. 10A2) and the level of evoked MUA was significantly ($P < 0.05$) reduced to $82.3 \pm 5\%$ ($n = 7$, Fig. 10A3). Accordingly, the power of the gamma component in the thalamic response was significantly ($P < 0.001$) reduced to $57.2 \pm 3.9\%$ ($n = 7$) when compared with the control responses obtained before cortical inactivation (Fig. 10A3). Similar results could be observed for the spontaneously occurring activity (Fig. 10B). After lidocaine application to the cortex, the occurrence of spontaneous thalamic bursts did not change significantly (0.93 ± 0.15 vs. 0.88 ± 0.18 min^{-1}, $n = 6$ P1 rats). However, the level of thalamic MUA within a burst was reduced to $64.1 \pm 14.2\%$ ($n = 6$) and the power of the gamma component of these spontaneous thalamic bursts was significantly ($n = 6$, $P < 0.01$) reduced to $55.2 \pm 7.3\%$, when compared with the controls (Fig. 10B3). These data indicate that already in P0–P1 rats, the cortex influences the properties of gamma burst activity in the thalamus, suggesting a cortical modulatory influence on the thalamic activity via cortico-thalamic feedback circuits at very early developmental stages.

Discussion

We show here for the first time that the rat barrel cortex in vivo reveals a precise topographic and functional columnar organization already at the day of birth. Although the graded expression of several transcription factors sets the rudimentary topography of thalamocortical connectivity, thereby specifying cortical areas and creating crude cortical maps during early prenatal stages (López-Bendito and Molnár 2003; O'Leary and Sahara 2008), our data indicate that spontaneously occurring and whisker stimulation-induced burst activity plays an important role in the formation of functional cortical columnar networks already before the cortex has gained its 6-layered structure. We demonstrate that gamma bursts synchronize local cortical networks into functional ontogenetic columns of 300–400 µm in diameter in the rat barrel cortex already at the day of birth and that the thalamus plays a central role in the generation of this cortical activity. Our data further indicate that a cortico-thalamic feedback loop modulates the thalamic spontaneously occurring and whisker stimulation-induced gamma burst activity already during neonatal stages of corticogenesis.

An important finding of our study is the precise cortical representation of single whiskers already in the first 2 postnatal days, even before all cortical layers have been formed—
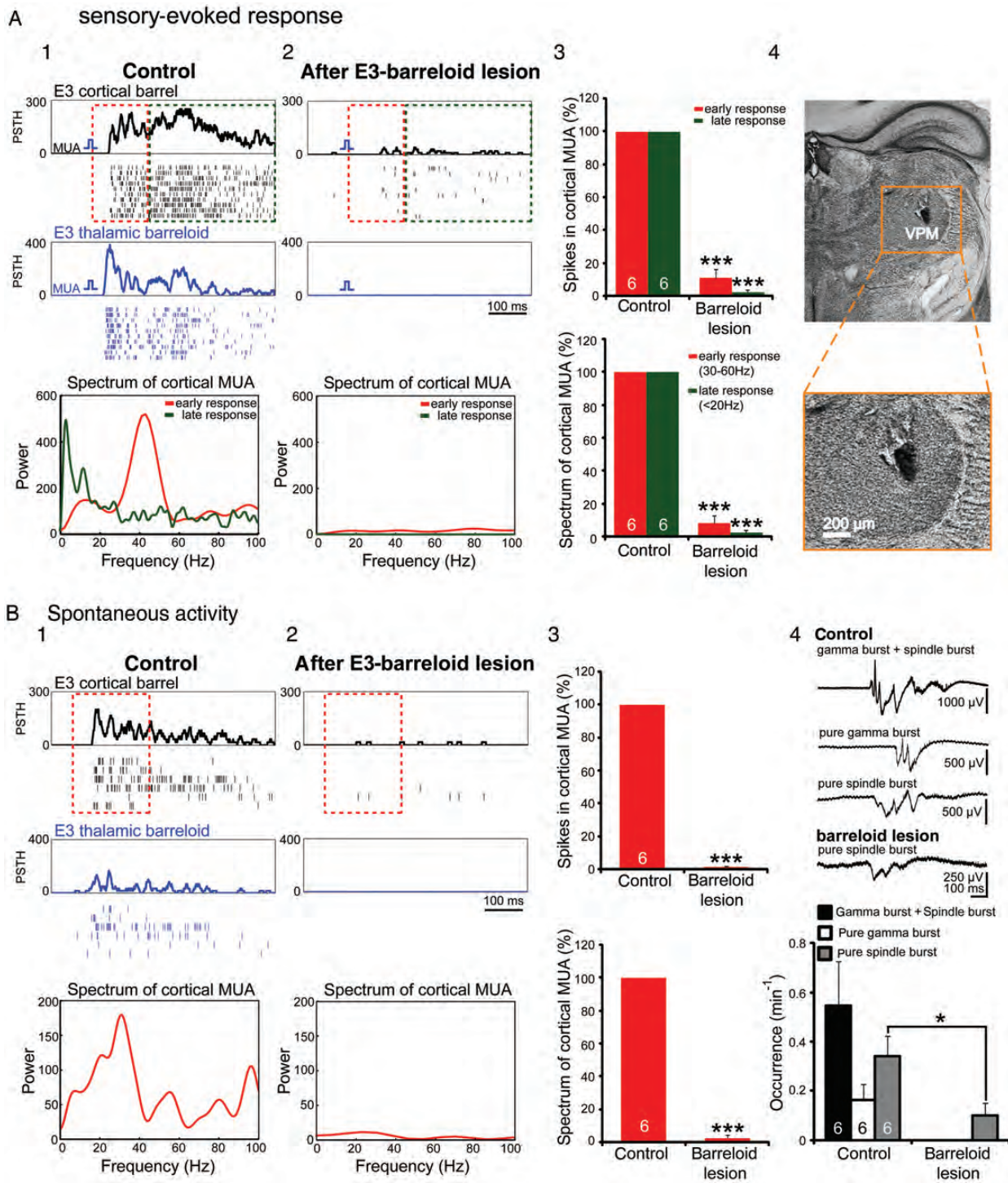
Figure 9. Local lesioning of the thalamus blocks whisker stimulation-induced and spontaneously occurring cortical gamma burst activity. (*A*) Control recordings of the MUA responses in the E3 cortical barrel (black) and thalamic barreloid (blue) to single-E3-whisker stimulation in a P1 rat with corresponding cortical MUA spectrum (early and late response) calculated from the data marked by red and green dashed line, respectively (*A1*). After an electrolytic lesion of the E3 thalamic barreloid, the cortical and thalamic responses to E3-whisker stimulation are almost completely blocked (*A2*). The pooled data from 6 P1 rats illustrating the relative number of cortical MUA spikes (top, shown as the proportion of MUA spikes relative to the value in the control period) and the power of the cortical MUA spectrum in the early (30–60 Hz) and late (<20 Hz) response (below) (*A3*). Note that both parameters were significantly reduced after local lesioning of the thalamus (***$P < 0.001$, paired t-test). The image of Nissl-stained coronal section from the same P1 rat showing the location and size of the electrolytic lesion in the VPM (*A4*). (*B*) Control recordings of spontaneous MUA in the barrel cortex and VPM of the same P1 rat as in panel A with corresponding cortical MUA spectrum calculated from the data marked by red dashed line (*B1*). The thalamic and cortical MUA raster plots and their corresponding poststimulus time histograms (PSTHs) were aligned to the onset of the cortical spontaneous events. After E3 barreloid lesioning, the MUA activity was markedly reduced in both the E3-pre-barrel-related column and the thalamic barreloid (*B2*), as also demonstrated in the power of the cortical MUA spectrum (bottom). The pooled data from 6 P1 rats illustrating the relative number of MUA spikes and the power of the MUA spectrum in the 30–60 Hz range (*B3*). Note that both parameters were significantly reduced after barreloid lesioning (***$P < 0.001$, paired t-test). Representative FPs of gamma and spindle bursts before and after barreloid lesioning (traces in top panel 4). After barreloid lesioning, the gamma containing spindle bursts and pure gamma bursts were completely blocked, and only pure spindle bursts were observed. The occurrence of pure spindle bursts was significantly (*$P \leq 0.05$, paired t-test) reduced (lower panel 4).
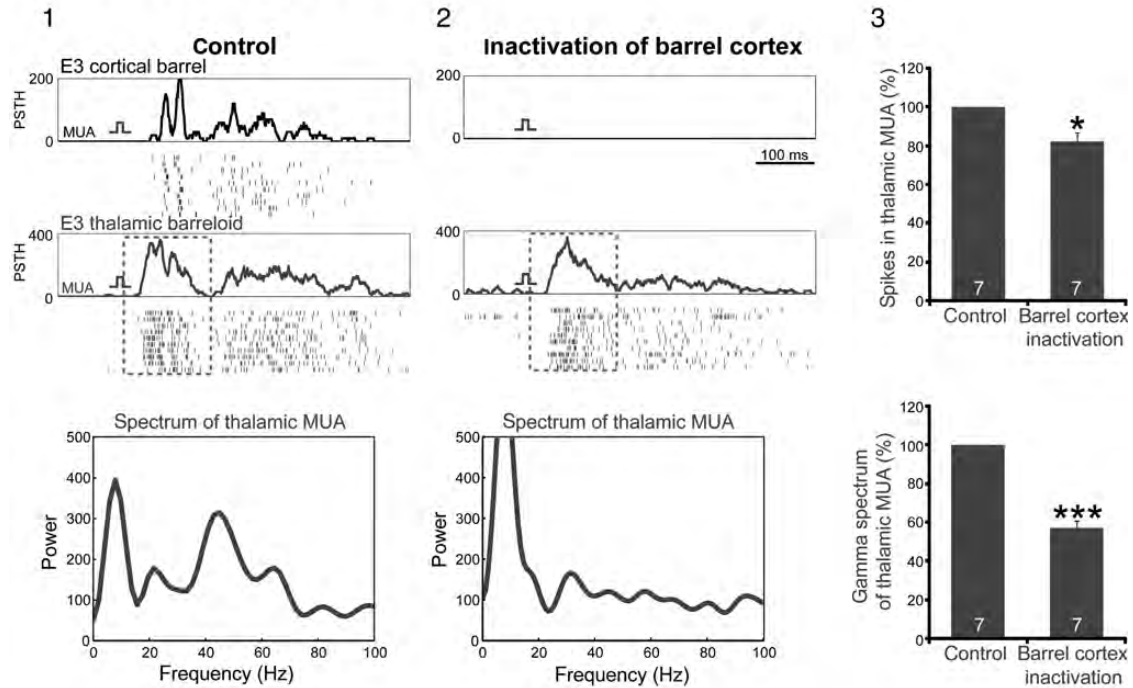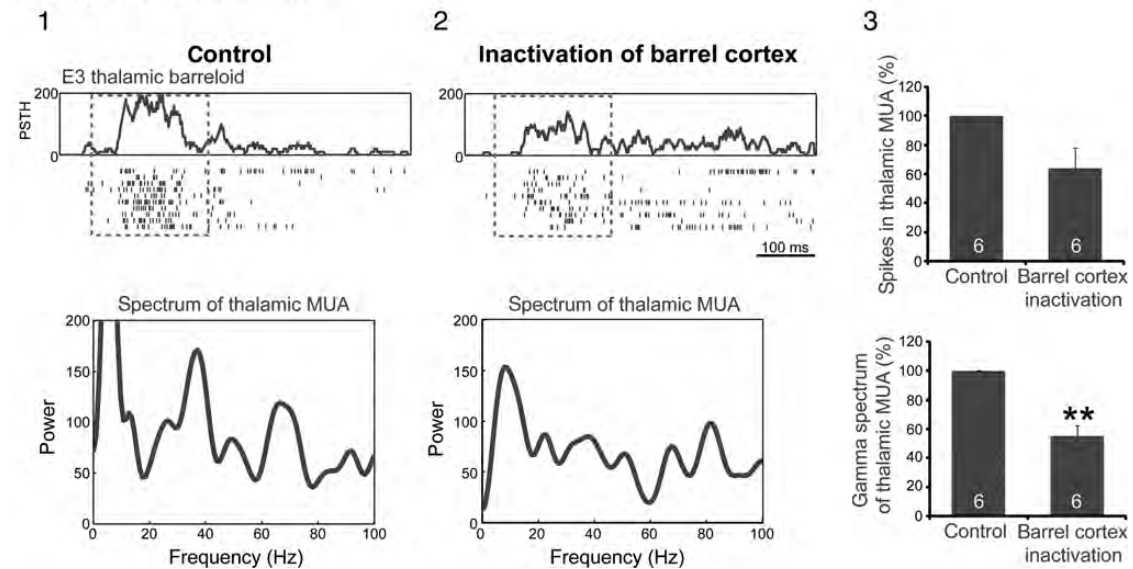
Figure 10. The cortical activity modulates thalamic gamma bursts. (A) MUA responses in the E3 cortical barrel (black) and thalamic barreloid (blue) to single-E3-whisker stimulation in a P1 rat with corresponding thalamic MUA spectrum and spike number calculated from the data marked by red dashed line (A1). After local inactivation of the barrel cortex with 1% lidocaine, the evoked MUA activity in the E3 barrel was completely blocked, whereas the activity in the thalamic barreloid was only slightly altered (A2). Note the prominent reduction of the gamma activity in the thalamus after inactivation of the cortex. The pooled data from 7 P0–P1 rats summarizing the effect of cortical inactivation on the number of thalamic MUA spikes (top) and gamma power (below) of evoked thalamic MUA activity (A3). Note the significant reduction of spike number and gamma activity in thalamic MUA after inactivation of the cortex (*$P < 0.05$, ***$P < 0.001$, paired t-test). (B) Control recordings of spontaneous MUA in the VPM of the same P1 rat as in panel A before (B1) and after local inactivation of the cortex with 1% lidocaine (B2). The thalamic MUA raster plots were aligned to the onset of the thalamic spontaneous events. The thalamic MUA spectrum was calculated from the data marked by red dashed line. Note the reduction in the 30–60 Hz range of the MUA spectrum after cortical inactivation. The pooled data from 6 P1 rats illustrating the effect of cortical inactivation on the number of spikes within the burst (top) and gamma power (below) of the spontaneous thalamic MUA activity (B3). Note that the power of the thalamic MUA spectrum in the 30–60 Hz range was significantly reduced (**$P < 0.01$, paired t-test).

a landmark which is reached at approximately P3 (Erzurumlu et al. 1990). We show that spontaneously occurring and whisker stimulation-induced cortical activity patterns correlate with the local thalamic activity and that local electrical stimulation of a single barreloid in the VPM elicited a cortical response that resembled in many aspects the sensory-evoked

cortical response following mechanical whisker stimulation, indicating the existence of a reliable thalamocortical connectivity and a precise topographic organization of the whisker to the barrel cortex pathway already at the day of birth. A surprisingly early segregation of ocular dominance columns have been previously also described in ferrets and cats before the thalamocortical afferents innervate layer IV, thus constituting the first component of a modular circuitry to emerge in the primary visual cortex (Crowley and Katz 2000).

In accordance with recent observations in P2–P7 rats (Minlebaev et al. 2011), our results show that already at P0–P1 the vast majority of evoked cortical responses consists of an early gamma burst, which synchronizes the cortical discharges. This synchronization in the gamma band may not only serve to code the properties of peripheral responses (Fries et al. 2007), but it is particularly suited to drive thalamocortical plasticity (Feldman et al. 1999; Minlebaev et al. 2011). It has been recently shown in the barrel cortex of P2–P4 rats that the gamma activity is generated independently from GABAergic interneurons via synchronized thalamic inputs (Minlebaev et al. 2011), in contrast to the more mature neocortex where GABAergic interneurons are essential (Mann et al. 2005). In line with this observation, our results also demonstrate the crucial role of the thalamus for the generation of gamma bursts already at the day of birth, even before all cortical layers have been formed approximately at P3. In vivo pharmacologic experiments in P1–P7 rats, the barrel cortex have indicated that spindle bursts are driven by glutamatergic synapses involving activation of AMPA and NMDA receptors, most likely resulting from the thalamocortical activity (Minlebaev et al. 2007, 2009).

Interestingly, in the present study, we obtained evidence for a modulatory feedback mechanism from the barrel cortex to the thalamus. Inactivation of the barrel cortex using local lidocaine application desynchronized spontaneously occurring and whisker stimulation-induced gamma burst activity in the VPM of P0–P1 rats. This desynchronization of the thalamic gamma activity suggests that cortico-thalamic efferents may considerably contribute to the synchronization of thalamic activity in the gamma frequency range. In some of our crosscorrelograms of the sensory-evoked gamma burst responses recorded simultaneously in both the thalamus and cortex of newborn rats, we obtained evidence for the existence of a cortico-thalamic feedback projection. Whereas a functional thalamocortical connection with relatively mature properties has been described in newborn rats (Hanganu et al. 2002), functional proof for the existence of a feedback cortico-thalamic projection is still lacking. However, a more detailed characterization of this projection is experimentally rather challenging and beyond the scope of the present study.

Another major finding of our study is that, under in vivo conditions, the thalamus plays a very important role in the generation of spontaneous cortical gamma and spindle bursts, which synchronize local neuronal networks (pre-barrel-related columns) in a topographic manner. The spontaneous neuronal activity has been recorded in the lateral geniculate nucleus of awake behaving ferrets before eye-opening (Weliky and Katz 1999), indicating that the thalamus can be involved in the initial patterning of neocortical circuits in the absence of sensory input. Our intrathalamic recordings of the spontaneous neuronal activity in the VPM of P0–P1 rats support this hypothesis. We show that the spontaneous

cortical gamma activity patterns always correlate with the local thalamic activity and that cortical gamma bursts evoked by local electrical stimulation of a single barreloid resembled in many aspects spontaneous gamma bursts. A local lesion in the VPM at the barreloid representing the stimulated whisker did not only block the sensory-evoked gamma burst response in the cortex, but also completely eliminated the spontaneous cortical gamma burst activity. These data indicate that the thalamus is required for the cortical gamma burst activity in vivo. In contrast, the occurrence of spontaneous thalamic gamma bursts is unaltered after inactivation of the barrel cortex using lidocaine, indicating that the cortex is not involved in the generation of the spontaneous thalamic activity. On the other hand, these experiments do not exclude the possibility that the spontaneously occurring activity recorded in the thalamus is triggered in the sensory periphery or in the trigeminal nuclei.

Evidence for an important role of the sensory periphery in driving spontaneously occurring activity in sensory cortical areas comes from the previous studies in the visual, auditory, and somatosensory system (for recent review, see Kilb et al. 2011). These reports strongly suggest that different sensory systems reveal similar mechanisms to drive early cortical networks although with a different developmental profile (Colonnese et al. 2010). Hanganu et al. (2006) performed simultaneous recordings from the retina and visual cortex of 1-week-old rats and demonstrated that spontaneous retinal bursts correlated with spindle bursts in the contralateral visual cortex. In the visual cortex of P10–P11 rats (before eye-opening), 87% of the spontaneous cortical activity was generated in the retina (Colonnese and Khazipov 2010). In the developing auditory system, supporting cells in the cochlea provide the stimulus responsible for initiating the spontaneous burst activity in auditory nerve fibers before the onset of hearing (Tritsch et al. 2007; Tritsch and Bergles 2010). This spontaneous peripheral activity probably plays an important role in the refinement and maintenance of synaptic connections and tonotopic maps in higher auditory structures. Khazipov et al. (2004) demonstrated in the somatosensory cortex of newborn rats that spatially confined spindle bursts are selectively triggered in a somatotopic manner by spontaneous muscle twitches, indicting a strong interference between sensory and motor systems. We have previously shown in newborn rats that transient peripheral deafferentation by the injection of lidocaine into the whisker pad causes a significant reduction in the occurrence of spontaneous cortical spindle bursts and gamma oscillations (Yang et al. 2009), indicating the important role of the sensory periphery for the generation of spontaneously occurring activity patterns also in the barrel cortex. Inactivation of the sensory periphery reduced the occurrence of gamma and spindle bursts by ~50% (Yang et al. 2009), while functional inactivation of thalamic barreloids in the present study completely abolished spontaneous cortical pure gamma bursts, gamma-containing spindle bursts and reduced the occurrence of spontaneous pure spindle bursts by ~75% (Fig. 9), indicating that a substantial portion of spontaneous gamma and spindle bursts may originate directly from the thalamus or the trigeminal nuclei and is not triggered in the sensory periphery.

On the other hand, there are still some pure spindle bursts which persisted after thalamic barreloid lesion. It is possible that the persistent pure spindle bursts, as other forms of

spontaneous early network oscillations (Garaschuk et al. 2000), are generated within the pre-barrel-related column itself. A number of studies have shown that the neonatal cerebral cortex has the intrinsic capacity to generate the local columnar activity patterns even without thalamocortical synaptic input. In vivo multi-electrode extracellular recordings in the developing ferret area 17 revealed an intrinsic patchy organization of patterned correlated activity at horizontal distances of ~1 mm, independent of the thalamic input activity (Chiu and Weliky 2001), and these patches correlated with early ocular dominance columns before eye-opening (Chiu and Weliky 2002). It is also possible that the persistent pure spindle bursts might originate from the neighboring pre-barrel-related column, because the spontaneous VSDI recordings showed that ~20–30% of the local spontaneous events can spread into the neighboring pre-barrel-related columns (Fig. 2). Another possibility is that the persistent pure spindle bursts originate from other non-thalamic subcortical inputs. For example, it has been shown that cholinergic inputs from the basal forebrain can facilitate spindle bursts in the neonatal rat primary visual cortex (Hanganu et al. 2007).

It has been previously shown in the newborn rat somatosensory cortex in vivo that the subplate is involved in the generation of the local cortical gamma and spindle burst activity (Yang et al. 2009). Furthermore, it has been recently reported that subplate neurons are required for the generation of spindle bursts activity in the limb region of the newborn rat somatosensory cortex in vivo and that removal of the subplate prevents the normal formation of the barrel field structure (Tolner et al. 2012). Under in vitro conditions, optical imaging and multi-electrode recordings in somatosensory cortical slices and intact cortex preparations have revealed subplate-driven local oscillatory networks and functional columnar units in newborn rodents (Yuste et al. 1992; Dupont et al. 2006; Sun and Luhmann 2007). Therefore, the subplate may be a central element in the generation of evoked and spontaneous gamma and spindle bursts during the early stages of cortical development. Before the formation of layer IV, thalamocortical inputs make functional synaptic connections with the subplate (Friauf et al. 1990; Hanganu et al. 2002) suggesting that in the first 2 postnatal days of rat development, subplate neurons are an essential element of thalamocortical information transfer (Luhmann et al. 2009; Kanold and Luhmann 2010).

In conclusion, our data indicate that the basic mosaic-like structure of the cortical columnar architecture develops very early (Luhmann et al. 1986), as initially proposed in the radial unit hypothesis of cortical development (Rakic 1988; Rakic et al. 2009). We suggest that spontaneous- and sensory-evoked burst activity plays an important role in the development of the cortical columnar architecture clearly before the onset of experience-dependent critical periods and identified the thalamus as a pivotal structure in the generation of spontaneous cortical gamma and spindle bursts, which synchronize local cortical networks into early barrel-related columns. Future studies may reveal interactions between these early electrical activity patterns and the expression of transcription factors in the developing cerebral cortex.

Supplementary Material

Supplementary material can be found at: http://www.cercor.oxfordjournals.org/.

References

Amaral DG, Schumann CM, Nordahl CW. 2008. Neuroanatomy of autism. Trends Neurosci. 31:137–145.

Berger T, Borgdorff A, Crochet S, Neubauer FB, Lefort S, Fauvet B, Ferezou I, Carleton A, Luscher HR, Petersen CC. 2007. Combined voltage and calcium epifluorescence imaging in vitro and in vivo reveals subthreshold and suprathreshold dynamics of mouse barrel cortex. J Neurophysiol. 97:3751–3762.

Bureau I. 2009. The development of cortical columns: role of Fragile X mental retardation protein. J Physiol. 587:1897–1901.

Bureau I, Shepherd GM, Svoboda K. 2008. Circuit and plasticity defects in the developing somatosensory cortex of FMR1 knock-out mice. J Neurosci. 28:5178–5188.

Chiu C, Weliky M. 2002. Relationship of correlated spontaneous activity to functional ocular dominance columns in the developing visual cortex. Neuron. 35:1123–1134.

Chiu C, Weliky M. 2001. Spontaneous activity in developing ferret visual cortex in vivo. J Neurosci. 21:8906–8914.

Colonnese MT, Kaminska A, Minlebaev M, Milh M, Bloem B, Lescure S, Moriette G, Chiron C, Ben Ari Y, Khazipov R. 2010. A conserved switch in sensory processing prepares developing neocortex for vision. Neuron. 67:480–498.

Colonnese MT, Khazipov R. 2010. "Slow activity transients" in infant rat visual cortex: a spreading synchronous oscillation patterned by retinal waves. J Neurosci. 30:4325–4337.

Crair MC, Gillespie DC, Stryker MP. 1998. The role of visual experience in the development of columns in cat visual cortex. Science. 279:566–570.

Crowley JC, Katz LC. 2000. Early development of ocular dominance columns. Science. 290:1321–1324.

Dupont E, Hanganu IL, Kilb W, Hirsch S, Luhmann HJ. 2006. Rapid developmental switch in the mechanisms driving early cortical columnar networks. Nature. 439:79–83.

Erzurumlu RS, Jhaveri S, Benowitz LI. 1990. Transient patterns of GAP-43 expression during the formation of barrels in the rat somatosensory cortex. J Comp Neurol. 292:443–456.

Feldman DE, Nicoll RA, Malenka RC. 1999. Synaptic plasticity at thalamocortical synapses in developing rat somatosensory cortex: LTP, LTD, and silent synapses. J Neurobiol. 41:92–101.

Fishell G, Kriegstein AR. 2003. Neurons from radial glia: the consequences of asymmetric inheritance. Curr Opin Neurobiol. 13:34–41.

Fox K. 2008. Barrel cortex. Cambridge: Cambridge University Press.

Friauf E, McConnell SK, Shatz CJ. 1990. Functional synaptic circuits in the subplate during fetal and early postnatal development of cat visual cortex. J Neurosci. 10:2601–2613.

Fries P, Nikolic D, Singer W. 2007. The gamma cycle. Trends Neurosci. 30:309–316.

Garaschuk O, Linn J, Eilers J, Konnerth A. 2000. Large-scale oscillatory calcium waves in the immature cortex. Nat Neurosci. 3:452–459.

Hanganu IL, Ben Ari Y, Khazipov R. 2006. Retinal waves trigger spindle bursts in the neonatal rat visual cortex. J Neurosci. 26:6728–6736.

Hanganu IL, Kilb W, Luhmann HJ. 2002. Functional synaptic projections onto subplate neurons in neonatal rat somatosensory cortex. J Neurosci. 22:7165–7176.

Hanganu IL, Staiger JF, Ben Ari Y, Khazipov R. 2007. Cholinergic modulation of spindle bursts in the neonatal rat visual cortex in vivo. J Neurosci. 27:5694–5705.

Hensch TK. 2005. Critical period plasticity in local cortical circuits. Nat Rev Neurosci. 6:877–888.

Hooks BM, Chen C. 2007. Critical periods in the visual system: changing views for a model of experience-dependent plasticity. Neuron. 56:312–326.

Hubel DH, Wiesel TN. 1962. Receptive fields, binocular interaction and functional architecture in the cat's visual cortex. J Physiol. 160:106–154.

Jones EG, Rakic P. 2010. Radial columns in cortical architecture: it is the composition that counts. Cereb Cortex. 20:2261–2264.

Kanold PO, Luhmann HJ. 2010. The subplate and early cortical circuits. Annu Rev Neurosci. 33:23–48.

Katz LC, Crowley JC. 2002. Development of cortical circuits: lessons from ocular dominance columns. Nat Rev Neurosci. 3:34–42.

Khazipov R, Sirota A, Leinekugel X, Holmes GL, Ben Ari Y, Buzsáki G. 2004. Early motor activity drives spindle bursts in the developing somatosensory cortex. Nature. 432:758–761.

Kilb W, Kirischuk S, Luhmann HJ. 2011. Electrical activity patterns and the functional maturation of the neocortex. Eur J Neurosci. 34:1677–1686.

Krupa DJ, Brisben AJ, Nicolelis MA. 2001. A multi-channel whisker stimulator for producing spatiotemporally complex tactile stimuli. J Neurosci Methods. 104:199–208.

Lahtinen H, Palva JM, Sumanen S, Voipio J, Kaila K, Taira T. 2002. Postnatal development of rat hippocampal gamma rhythm in vivo. J Neurophysiol. 88:1469–1474.

López-Bendito G, Molnár Z. 2003. Thalamocortical development: how are we going to get there? Nat Rev Neurosci. 4:276–289.

Luhmann HJ, Kilb W, Hanganu-Opatz IL. 2009. Subplate cells: amplifiers of neuronal activity in the developing cerebral cortex. Front Neuroanat. 3:19.

Luhmann HJ, Martinez ML, Singer W. 1986. Development of horizontal intrinsic connections in cat striate cortex. Exp Brain Res. 63:443–448.

Mann EO, Suckling JM, Hajos N, Greenfield SA, Paulsen O. 2005. Perisomatic feedback inhibition underlies cholinergically induced fast network oscillations in the rat hippocampus in vitro. Neuron. 45:105–117.

Marcano-Reik AJ, Prasad T, Weiner JA, Blumberg MS. 2010. An abrupt developmental shift in callosal modulation of sleep-related spindle bursts coincides with the emergence of excitatory-inhibitory balance and a reduction of somatosensory cortical plasticity. Behav Neurosci. 124:600–611.

Minlebaev M, Ben Ari Y, Khazipov R. 2007. Network mechanisms of spindle-burst oscillations in the neonatal rat barrel cortex in vivo. J Neurophysiol. 97:692–700.

Minlebaev M, Ben Ari Y, Khazipov R. 2009. NMDA receptors pattern early activity in the developing barrel cortex in vivo. Cereb Cortex. 19:688–696.

Minlebaev M, Colonnese M, Tsintsadze T, Sirota A, Khazipov R. 2011. Early gamma oscillations synchronize developing thalamus and cortex. Science. 334:226–229.

Mountcastle VB. 1997. The columnar organization of the neocortex. Brain. 120:701–722.

Mountcastle VB. 1957. Modality and topographic properties of single neurons of cat's somatic sensory cortex. J Neurophysiol. 20:408–434.

Noctor SC, Flint AC, Weissman TA, Dammerman RS, Kriegstein AR. 2001. Neurons derived from radial glial cells establish radial units in neocortex. Nature. 409:714–720.

O'Leary DD, Sahara S. 2008. Genetic regulation of arealization of the neocortex. Curr Opin Neurobiol. 18:90–100.

Paxinos G, Watson C. 1998. The rat brain in stereotaxic coordinates. San Diego: Academic Press.

Petersen CC. 2007. The functional organization of the barrel cortex. Neuron. 56:339–355.

Rakic P. 1988. Specification of cerebral cortical areas. Science. 241:170–176.

Rakic P, Ayoub AE, Breunig JJ, Dominguez MH. 2009. Decision by division: making cortical maps. Trends Neurosci. 32:291–301.

Ratzlaff EH, Grinvald A. 1991. A tandem-lens epifluorescence macroscope: hundred-fold brightness advantage for wide-field imaging. J Neurosci Methods. 36:127–137.

Sun JJ, Luhmann HJ. 2007. Spatio-temporal dynamics of oscillatory network activity in the neonatal mouse cerebral cortex. Eur J Neurosci. 26:1995–2004.

Tolner EA, Sheikh A, Yukin AY, Kaila K, Kanold PO. 2012. Subplate neurons promote spindle bursts and thalamocortical patterning in the neonatal rat somatosensory cortex. J Neurosci. 32:692–702.

Tritsch NX, Bergles DE. 2010. Developmental regulation of spontaneous activity in the mammalian cochlea. J Neurosci. 30:1539–1550.

Tritsch NX, Yi E, Gale JE, Glowatzki E, Bergles DE. 2007. The origin of spontaneous activity in the developing auditory system. Nature. 450:50–55.

Wang XJ, Buzsáki G. 1996. Gamma oscillation by synaptic inhibition in a hippocampal interneuronal network model. J Neurosci. 16:6402–6413.

Weliky M, Katz LC. 1999. Correlational structure of spontaneous neuronal activity in the developing lateral geniculate nucleus in vivo. Science. 285:599–604.

Woolsey TA, Van der LH. 1970. The structural organization of layer IV in the somatosensory region (SI) of mouse cerebral cortex. The description of a cortical field composed of discrete cytoarchitectonic units. Brain Res. 17:205–242.

Yang JW, Hanganu-Opatz IL, Sun JJ, Luhmann HJ. 2009. Three patterns of oscillatory activity differentially synchronize developing neocortical networks in vivo. J Neurosci. 29:9011–9025.

Yu YC, Bultje RS, Wang X, Shi SH. 2009. Specific synapses develop preferentially among sister excitatory neurons in the neocortex. Nature. 458:501–504.

Yuste R, Peinado A, Katz LC. 1992. Neuronal domains in developing neocortex. Science. 257:665–669.